OXFORD CENTRE FOR COLLABORATIVE APPLIED MATHEMATICS

Report Number 10/60

Stochastic synchronization of neuronal populations with intrinsic and extrinsic noise

by

Paul C. Bressloff and Yi Ming Lai

Oxford Centre for Collaborative Applied Mathematics
Mathematical Institute
24 - 29 St Giles'
Oxford
OX1 3LB
England

Stochastic synchronization of neuronal populations with intrinsic and extrinsic noise

Paul C. Bressloff[1,2] and Yi Ming Lai[1]

[1]Mathematical Institute, University of Oxford, 24-29 St. Giles', Oxford OX1 3LB, UK

[2] Department of Mathematics, University of Utah, 155 South 1400 East, Salt Lake City, Utah 84112, USA

November 5, 2010

Abstract

We extend the theory of noise–induced phase synchronization to the case of a neural master equation describing the stochastic dynamics of interacting excitatory and inhibitory populations of neurons (E-I networks). The master equation formulation of stochastic neurodynamics represents the state of each population by the number of currently active neurons, and the state transitions are chosen such that deterministic Wilson–Cowan rate equations are recovered in the mean–field limit. Assuming that each deterministic E-I network acts as a limit cycle oscillator, we combine phase reduction and averaging methods in order to determine the stationary distribution of phase differences in an ensemble of uncoupled E-I oscillators, and use this to explore how intrinsic noise disrupts synchronization due to a common extrinsic noise source. Finally, we show how a similar analysis can be carried out for another simple population model that exhibits limit cycle oscillations in the deterministic limit, namely, a recurrent excitatory network with synaptic depression; inclusion of intrinsic noise leads to a stochastic hybrid system.

1 Introduction

Synchronous oscillations are prevalent in many areas of the brain including sensory cortices, thalamus and hippocampus [15]. Recordings of population activity based on the electroencephalogram (EEG) or the local field potential (LFP) often exhibit strong peaks in the power spectrum at certain characteristic frequencies. For example, in the visual system of mammals, cortical oscillations in the γ frequency band (20-70 Hz) are generated with a spatially distributed phase that is modulated by the nature of a visual stimulus. Stimulus–induced phase synchronization of different populations of neurons has been proposed as a potential solution to the binding problem, that is, how various components of a visual image are combined into a single coherently perceived object [58, 29]. An alternative suggestion is that such oscillations provide a mechanism for attentionally gating the flow of neural information [55, 59]. Neuronal oscillations may be generated by intrinsic properties of single cells or may arise through excitatory and inhibitory synaptic interactions within a local population of cells. Irrespective of the identity of the basic oscillating unit, synchronization can occur via mutual interactions between the oscillators or via entrainment to a common periodic stimulus in the absence of coupling.

From a dynamical systems perspective, self–sustained oscillations in biological, physical and chemical systems are often described in terms of limit cycle oscillators where the timing along each limit cycle is specified in terms of a single phase variable. The phase–reduction method can then be used to analyze synchronization of an ensemble of oscillators by approximating the high–dimensional limit cycle dynamics as a closed system of equations for the corresponding phase variables [37, 20]. Although the phase–reduction method has traditionally been applied to deterministic limit cycle oscillators, there is growing interest in extending the method to take into account the effects of noise, in particular, the phenomenon of noise–induced phase synchronization [53, 64, 27, 22, 49, 45, 65, 43]. This concerns the counterintuitive idea that an ensemble of independent oscillators can be synchronized by a randomly fluctuating input applied globally to all of the oscillators. Evidence for such an effect has been found in experimental studies of oscillations in the olfactory bulb [22]. It is also suggested by the related phenomenon of spike-time reliability, in which the reproducibility of a single neuron's output spike train across trials is greatly enhanced by a fluctuating input when compared to a constant input [44, 23].

In this paper we extend the theory of noise–induced phase synchronization to the case of a neural master equation describing the stochastic dynamics of interacting excitatory and inhibitory populations of neurons. The master equation formulation of stochastic neurodynamics represents the state of each population by the number of currently active neurons, and the state transitions are chosen such that deterministic Wilson–Cowan rate equations [69, 70] are recovered in an appropriate mean–field limit (where statistical correlations can be neglected)

[51, 13, 14, 8]. We will consider the particular version of the neural master equation introduced by Bressloff [8], in which the state transition rates scale with the size N of each population in such a way that the Wilson–Cowan equations are obtained in the thermodynamic limit $N \to \infty$. Thus, for large but finite N, the network operates in a regime characterized by Gaussian–like fluctuations about attracting solutions (metastable states) of the mean–field equations (at least away from critical points), combined with rare transitions between different metastable states [9]. [In contrast, the master equation of Buice *et. al.* assumes that the network operates in a Poisson–like regime at the population level [13, 14]]. The Gaussian–like statistics can be captured by a corresponding neural Langevin equation that is obtained by carrying out a Kramers–Moyal expansion of the master equation [24]. One motivation for the neural master equation is that it represents an intrinsic noise source at the network level arising from finite size effects. That is, a number of studies of fully or sparsely connected integrate–and–fire networks have shown that under certain conditions, even though individual neurons exhibit Poisson–like statistics, the neurons fire asynchronously so that the total population activity evolves according to a mean–field rate equation [1, 25, 11, 10, 54]. However, formally speaking, the asynchronous state only exists in the thermodynamic limit $N \to \infty$, so that fluctuations about the asynchronous state arise for finite N [48, 46, 61, 7]. (Finite-size effects in IF networks have also been studied using linear response theory [18]).

For concreteness, we focus on one of the simplest networks known to generate limit cycle oscillations at the population level, namely, a pair of mutually coupled excitatory (E) and inhibitory (I) populations [6]. A number of modeling studies of stimulus–induced oscillations and synchrony in primary visual cortex have taken the basic oscillatory unit to be an E-I network operating in a limit cycle regime [60, 28]. The E-I network represents a cortical column, which can synchronize with other cortical columns either via long-range synaptic coupling or via a common external drive. In this paper, we investigate to what extent a common external stochastic drive can synchronize an ensemble of uncoupled E-I oscillators, each of which has uncorrelated intrinsic noise. In particular, we extend stochastic phase reduction methods developed to analyze noise–induced synchronization of uncoupled limit cycle oscillators [64, 22, 49, 45, 65, 43] so that we can take into account the effects of intrinsic noise. The structure of the paper is as follows. The basic master equation formulation of stochastic neurodynamics is presented in section 2, where we also derive the corresponding neural Langevin equation. In section 3 we introduce the E-I model and show how intrinsic noise can amplify subthresold oscillations (quasicycles). This is achieved by considering the power spectrum of the neural Langevin equation along analogous lines to a recent study of biochemical oscillators [47, 5]. In section 4 we carry out the stochastic phase reduction of a single E-I network, taking care to distinguish between the Ito and Stratonovich versions of stochastic calculus [24]. We use this to characterize the

effects of intrinsic noise on the mean period and variance of the oscillations. In section 5, we combine phase reduction and averaging methods along the lines of Nakao *et. al.* [49] in order to determine the stationary distribution of phase differences in an ensemble of uncoupled E-I oscillators, and use this to explore how intrinsic noise disrupts synchronization due to a common extrinsic noise source. Finally, in section 6 we show how a similar analysis can be carried out for another population model that exhibits limit cycle oscillations in the deterministic limit, namely, an excitatory recurrent network with synaptic depression; such a network forms the basis of various studies of spontaneous synchronous oscillations in cortex [62, 63, 31, 34, 35]. The inclusion of intrinsic noise leads to a stochastic hybrid system [52].

2 Neural Langevin equation

Suppose that there exist M homogeneous neuronal populations labeled $i = 1, \ldots, M$, each consisting of N neurons[1]. Assume that all neurons of a given population are equivalent in the sense that the pairwise synaptic interaction between a neuron of population i and a neuron of population j only depends on i and j. Each neuron can be in either an active or quiescent state. Let $N_i(t)$ denote the number of active neurons at time t. The state or configuration of the network is then specified by the vector $\mathbf{N}(t) = (N_1(t), N_2(t), \ldots, N_M(t))$, where each $N_i(t)$ is treated as a discrete stochastic variable that evolves according to a one–step jump Markov process. Let $P(\mathbf{n}, t) = \text{Prob}[\mathbf{N}(t) = \mathbf{n}]$ denote the probability that the network of interacting populations has configuration $\mathbf{n} = (n_1, n_2, \ldots, n_M)$ at time $t, t > 0$, given some initial distribution $P(\mathbf{n}, 0)$. The probability distribution is taken to evolve according to a master equation of the form [51, 13, 14, 8]

$$\frac{dP(\mathbf{n},t)}{dt} = \sum_{k=1}^{M} \sum_{r=\pm 1} \left[T_{k,r}(\mathbf{n} - r\mathbf{e}_k) P(\mathbf{n} - r\mathbf{e}_k, t) - T_{k,r}(\mathbf{n}) P(\mathbf{n}, t) \right]. \tag{2.1}$$

with boundary condition $P(\mathbf{n}, t) \equiv 0$ if $n_i = -1$ for some i. Here $\mathbf{e}_k$ denotes the unit vector whose kth component is equal to unity. The corresponding transition rates are chosen so that in the thermodynamic limit $N \to \infty$ one recovers the deterministic Wilson-Cowan equations [69, 70] (see below):

$$T_{k,-1}(\mathbf{n}) = \alpha_k n_k, \; T_{k,+1}(\mathbf{n}) = NF\left(\sum_l w_{kl} n_l / N + I_k \right). \tag{2.2}$$

[1]One could take the number of neurons in each population to be different provided that they all scaled with N. For example, one could identify the system size parameter N with the mean number of synaptic connections into a neuron in a sparsely coupled network.

where α_k are rate constants, w_{kl} is the effective synaptic weight from the lth to the kth population, and I_k are external inputs. The gain function F is taken to be the sigmoid function

$$F(x) = \frac{F_0}{1 + \mathrm{e}^{-\gamma x}}, \tag{2.3}$$

with gain γ and maximum firing rate F_0. (Any threshold can be absorbed into the external inputs I_k). Equation (2.1) preserves the normalization condition $\sum_{n_1 \geq 0} \ldots \sum_{n_M \geq 0} P(\mathbf{n}, t) = 1$ for all $t \geq 0$. The master equation given by equations (2.1) and (2.2) is a phenomenological representation of stochastic neurodynamics [51, 8]. It is motivated by various studies of noisy spiking networks which show that under certain conditions, even though individual neurons exhibit Poisson–like statistics, the neurons fire asynchronously so that the population activity can be characterized by fluctuations around a mean rate evolving according to a deterministic mean–field equation [1, 25, 11, 10]. On the other hand, if population activity is itself Poisson–like, then it is more appropriate to consider an N–independent version of the master equation, in which $NF \to F$ and $\mathbf{w}/N \to \mathbf{w}$ [13, 14]. The advantage of our choice of scaling from an analytical viewpoint is that one can treat N^{-1} as a small parameter and use perturbation methods such as the Kramers-Moyal expansion to derive a corresponding neural Langevin equation [33].

Multiplying both sides of the master equation (2.1) by n_k followed by a summation over all configuration states leads to

$$\frac{d}{dt}\langle n_k \rangle = \sum_{r=\pm 1} r \langle T_{k,r}(\mathbf{n}) \rangle, \tag{2.4}$$

where the brackets $\langle \ldots \rangle$ denote a time–dependent ensemble averaging over realization of the stochastic dynamics, that is, $\langle f(\mathbf{n}) \rangle = \sum_{\mathbf{n}} P(\mathbf{n}, t) f(\mathbf{n})$ for any function of state $f(\mathbf{n})$. We now impose the mean–field approximation $\langle T_{k,r}(\mathbf{n}) \rangle \approx T_{k,r}(\langle \mathbf{n} \rangle)$, which is based on the assumption that statistical correlations can be neglected. Introducing the mean activity variables $\bar{x}_k = N^{-1}\langle n_k \rangle$ means that we can write the resulting mean–field equations in the form

$$\frac{d}{dt}\bar{x}_k = N^{-1}[T_{k,+}(N\bar{\mathbf{x}}) - T_{k,-}(N\bar{\mathbf{x}})] \equiv H_k(\bar{\mathbf{x}}) \tag{2.5}$$

Substituting for $T_{k,r}$ using equation (2.2) yields the deterministic Wilson–Cowan equations [70]

$$\frac{d\bar{x}_k}{dt} = -\alpha_k \bar{x}_k + F\left(\sum_l w_{kl}\bar{x}_l + I_k\right). \tag{2.6}$$

Strictly speaking, the mean–field description is only valid in the thermodynamic limit $N \to \infty$, and provided that this limit is taken before the limit $t \to \infty$ [9]. In this paper we are interested in the effects of intrinsic noise fluctuations arising from the fact that each neural population is finite.

Let us introduce the rescaled variables $x_k = n_k/N$ and corresponding transition rates

$$\Omega_{k,-1}(\mathbf{x}) = \alpha_k x_k,\ \Omega_{k,1}(\mathbf{x}) = F\left(\sum_l w_{kl}x_l + I_k\right). \tag{2.7}$$

Equation (2.1) can then be rewritten in the form

$$\frac{dP(\mathbf{x},t)}{dt} = N\sum_{k=1}^{M}\sum_{r=\pm 1}\left[\Omega_{k,r}(\mathbf{x}-r\mathbf{e}_k/N)P(\mathbf{x}-r\mathbf{e}_k/N,t) - \Omega_{k,r}(\mathbf{x})P(\mathbf{x},t)\right]. \tag{2.8}$$

Treating x_k as a continuous variable and Taylor expanding terms on the right–hand side to second order in N^{-1} leads to the Fokker–Planck equation

$$\frac{\partial P(\mathbf{x},t)}{\partial t} = -\sum_{k=1}^{M}\frac{\partial}{\partial x_k}\left[A_k(\mathbf{x})P(\mathbf{x},t)\right] + \frac{\epsilon^2}{2}\sum_{k=1}^{M}\frac{\partial^2}{\partial x_k^2}\left[B_k(\mathbf{x})P(\mathbf{x},t)\right] \tag{2.9}$$

with $\epsilon = N^{-1/2}$,

$$A_k(\mathbf{x}) = \Omega_{k,1}(\mathbf{x}) - \Omega_{k,-1}(\mathbf{x}) \tag{2.10}$$

and

$$B_k(\mathbf{x}) = \Omega_{k,1}(\mathbf{x}) + \Omega_{k,-1}(\mathbf{x}). \tag{2.11}$$

The solution to the Fokker–Planck equation (2.9) determines the probability density function for a corresponding stochastic process $\mathbf{X}(t) = (X_1(t),\ldots,X_M(t))$, which evolves according to a neural Langevin equation of the form

$$dX_k = A_k(\mathbf{X})dt + \epsilon b_k(\mathbf{X})dW_k(t). \tag{2.12}$$

with $b_k(\mathbf{x})^2 = B_k(\mathbf{x})$. Here $W_k(t)$ denotes an independent Wiener process such that

$$\langle dW_k(t)\rangle = 0, \quad \langle dW_k(t)dW_l(t)\rangle = \delta_{k,l}dt. \tag{2.13}$$

Equation (2.12) is the neural analog of the well known chemical Langevin equation [26, 40]. (A rigorous analysis of the convergence of solutions of a chemical master equation to solutions of the corresponding Langevin equation in the mean–field limit has been carried out by Kurtz [38]). It is important to note that the Langevin equation (2.12) takes the form of an Ito rather than Stratonovich stochastic differential equation (SDE). This distinction will be important in our subsequent analysis (see section 4).

The above neural Langevin equation approximates the effects of intrinsic noise fluctuations when the number N of neurons in each population is large but finite. It is also possible to extend the neural Langevin equation to incorporate the effects of a common extrinsic noise source, which will be used to analyze noise–induced synchronization in section 5. In particular,

suppose that the external drive I_k to the kth population can be decomposed into a deterministic part and a stochastic part according to

$$I_k = h_k + \frac{2\sigma\chi_k}{\sqrt{F_0}}\xi(t), \tag{2.14}$$

where h_k is a constant input and $\xi(t)$ is a white noise term, which is assumed to be common to all the neural populations; the level of extrinsic noise is given by the dimensionless quantity σ and $\sum_{k=1}^{M}\chi_k = 1$. Substituting for I_k in equation (2.7) and assuming that σ is sufficiently small, we can Taylor expand $\Omega_{k,1}$ to first order in σ to give

$$\Omega_{k,1}(\mathbf{x}) \approx F(\sum_l w_{kl}x_l + h_k) + \frac{2\sigma\chi_k}{\sqrt{F_0}}F'(\sum_l w_{kl}x_l + h_k)\xi(t). \tag{2.15}$$

Carrying out a corresponding expansion of the drift function $A_k(\mathbf{x})$ then leads to the extended neural Langevin equation

$$dX_k = A_k(\mathbf{X})dt + \epsilon b_k(\mathbf{X})dW_k(t) + \sigma a_k(\mathbf{X})dW(t), \tag{2.16}$$

where

$$a_k(\mathbf{x}) = 2\chi_k F'(\sum_l w_{kl}x_l + h_k)/\sqrt{F_0} \tag{2.17}$$

and $dW(t) = \xi(t)dt$ is an additional independent Wiener process that is common to all populations. We now have a combination of intrinsic noise terms that are treated in the sense of Ito, and an extrinsic noise term that is treated in the sense of Stratonovich. The latter is based on the physical assumption that external sources of noise have finite correlation times, so that we are considering the external noise to be the zero correlation time limit of a colored noise process.

3 Noise-induced amplification of oscillations in an E-I network

Consider a two–population model consisting of an excitatory population interacting with an inhibitory population as shown in Fig. 1. The associated mean–field equation (2.6) for this so–called E-I network reduces to the pair of equations (dropping the bar on $\bar{x}_k$)

$$\begin{aligned}\frac{dx_E}{dt} &= -x_E + F\left(w_{EE}x_E + w_{EI}x_I + h_E\right)\\ \frac{dx_I}{dt} &= -x_I + F\left(w_{IE}x_E + w_{II}x_I + h_I\right),\end{aligned} \tag{3.1}$$

where we have set $\alpha_{E,I} = \alpha = 1$ for simplicity. (We interpret α^{-1} as a membrane time constant and take $\alpha^{-1} = 10$ msec in physical units). Also note that $w_{EE}, w_{IE} \geq 0$ and $w_{EI}, w_{II} \leq 0$. The bifurcation structure of the two–population Wilson–Cowan model given by equations (3.1)

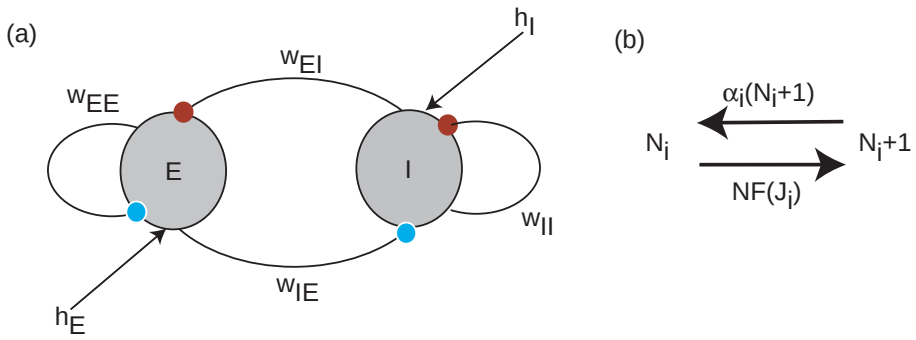

Figure 1: Stochastic Wilson–Cowan model of an E-I network. (a) Two–population network consisting of N excitatory neurons interacting with N inhibitory neurons. The state of the ith population ($i = E, I$) is specified by the number N_i of spikes generated within the population over a single time bin. The synaptic weights w_{ij} and external inputs h_i determine the total synaptic input according to $J_i = \sum_{j=E,i} w_{ij} m_j/N + h_i$. (b) State transition diagram for underlying Markov process.

has been analyzed in detail elsewhere [6]. An equilibrium (x_E^*, x_I^*) is obtained as a solution of the pair of equations

$$\begin{aligned} x_E^* &= F\left(w_{EE}x_E^* + w_{EI}x_I^* + h_E\right) \\ x_I^* &= F\left(w_{IE}x_E^* + w_{II}x_I^* + h_I\right). \end{aligned} \tag{3.2}$$

These can be inverted to yield

$$\begin{aligned} h_E &= F^{-1}(x_E^*) - w_{EE}x_E^* - w_{EI}x_I^* \\ h_I &= F^{-1}(x_I^*) - w_{IE}x_E^* - w_{II}x_I^*. \end{aligned} \tag{3.3}$$

The associated Jacobian is

$$\mathbf{J} = \begin{pmatrix} -1 + w_{EE}F'\left(w_{EE}x_E^* + w_{EI}x_I^* + h_E\right) & w_{EI}F'\left(w_{EE}x_E^* + w_{EI}x_I^* + h_E\right) \\ w_{IE}F'\left(w_{IE}x_E^* + w_{II}x_I^* + h_I\right) & -1 + w_{II}F'\left(w_{IE}x_E^* + w_{II}x_I^* + h_I\right) \end{pmatrix}. \tag{3.4}$$

As a further simplification, let us take the gain function F to be the simple sigmoid $F(u) = (1 + \mathrm{e}^{-u})^{-1}$, that is, $F_0 = 1$ and $\gamma = 1$ in equation (2.3). Using the fact that the sigmoid function satisfies $F' = F(1 - F)$ and applying the fixed point equations allows us to represent the Jacobian in the simpler form

$$\mathbf{J} = \begin{pmatrix} -1 + w_{EE}x_E^*(1 - x_E^*) & w_{EI}x_E^*(1 - x_E^*) \\ w_{IE}x_I^*(1 - x_I^*) & -1 + w_{II}x_I^*(1 - x_I^*) \end{pmatrix}. \tag{3.5}$$

An equilibrium will be stable provided that the eigenvalues $\lambda_\pm$ of $\mathbf{J}$ have negative real parts, where

$$\lambda_\pm = \frac{1}{2}\left(\mathrm{Tr}\,\mathbf{J} \pm \sqrt{[\mathrm{Tr}\,\mathbf{J}]^2 - 4\mathrm{Det}\,\mathbf{J}}\right). \tag{3.6}$$

This leads to the stability conditions $\mathbf{Tr}\,\mathbf{J} < 0$ and $\mathrm{Det}\,\mathbf{J} > 0$. In order to construct a phase diagram in the (h_E, h_I)–plane for a fixed weight matrix $\mathbf{w}$, we express x_I^* as a function of x_E^* by imposing a constraint on the eigenvlaues $\lambda_\pm$ and then substitute the resulting function into equations (3.3). This yields bifurcation curves in the (h_E, h_I)–plane that are parameterized by x_E^*, $0 < x_E^* < 1$, see Fig. 2. For example, the constraint

$$\mathrm{Tr}\,\mathbf{J} \equiv -2 + w_{EE}x_E^*(1 - x_E^*) + w_{II}x_I^*(1 - x_I^*) = 0 \tag{3.7}$$

with $\mathrm{Det}\,\mathbf{J} > 0$ determines Hopf bifurcation curves where a pair of complex conjugate eigenvalues cross the imaginary axis. Since the trace is a quadratic function of x_E^*, x_I^*, obtain two Hopf branches. Similarly, the constraint $\mathrm{Det}\,\mathbf{J} = 0$ with $\mathrm{Tr}\,\mathbf{J} < 0$ determines saddle–node or fold bifurcation curves where a single real eigenvalue crosses zero. The saddle–node curves have to be determined numerically, since the determinant is a quartic function of x_E^*, x_I^*.

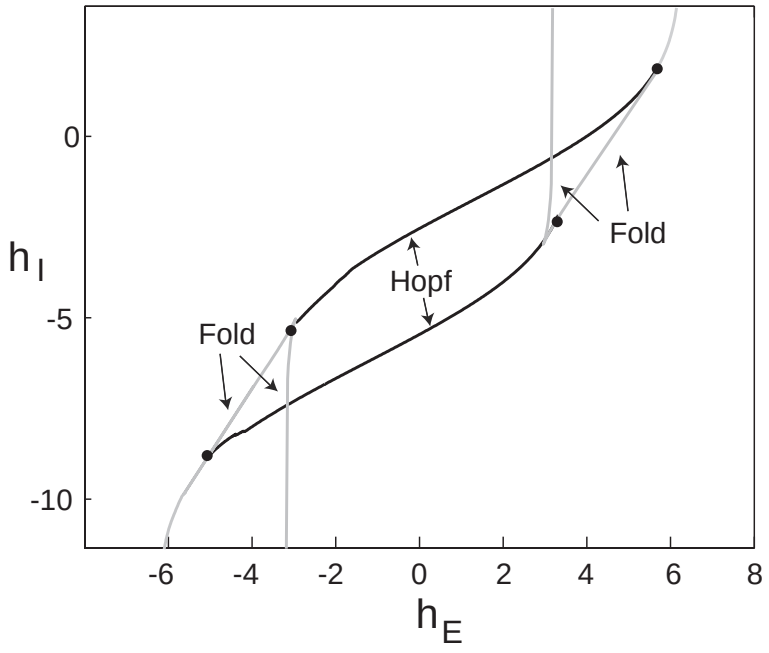

Figure 2: Phase diagram of two–population Wilson–Cowan model (3.1) for fixed set of weights $w_{EE} = 11.5, w_{IE} = -w_{EI} = 10$, $w_{II} = -2$. Also $F_0 = \gamma = 1$. The dots correspond to Takens–Bogdanov bifurcation points

In this paper, we will focus on the effects of noise when the deterministic E-I network acts

as a limit cycle oscillator. However, it is useful to briefly discuss the case of noise–induced oscillations or quasicycles, see also Ref. [9]. Therefore, suppose that the E-I network operates in a parameter regime where there exists a single fixed point of the mean–field equations (3.1). If the fixed point is a stable focus so that its Jacobian has a pair of complex conjugate eigenvalues, the corresponding deterministic network exhibits transient or subthreshold oscillations that decay at a rate given by the real part of the eigenvalues. Proceeding along similar lines to recent work on biochemical oscillations in cellular systems [47, 5], we will show how intrinsic noise can convert these transient oscillations into large amplitude sustained coherent oscillations, giving rise to a peak in the corresponding power spectrum (quasicycles). First, we decompose the solution to the neural Langevin equation (2.12) as

$$X_k = x_k^* + \epsilon \eta_k(t) \tag{3.8}$$

such that $A_k(\mathbf{x}^*) = 0$. Taylor expanding equation (2.12) to first order in ϵ then implies that η_k satisfies the linear Langevin equation

$$d\eta_k = \sum_{l=E,I} J_{kl}\eta_l dt + b_k(\mathbf{x}^*)dW_k(t), \tag{3.9}$$

where $J_{kl} = \partial A_k/\partial x_l|_{\mathbf{x}=\mathbf{x}^*}$. Introducing the white noise processes $\xi_k(t)$ according to $dW_k(t) = \xi_k(t)dt$ with

$$\langle \xi_k(t) \rangle = 0, \quad \langle \xi_k(t)\xi_l(t') \rangle = \delta_{k,l}\delta(t-t'), \tag{3.10}$$

we can rewrite the Langevin equation in the form

$$\frac{d\eta_k}{dt} = \sum_{l=E,I} J_{kl}\eta_l + b_k(\mathbf{x}^*)\xi_k(t), \tag{3.11}$$

Let $\widetilde{\eta}_k(\omega)$ denote the Fourier transform of $\eta(t)$ with

$$\widetilde{\eta}_k(\omega) = \int_{-\infty}^{\infty} \mathrm{e}^{-i\omega t}\eta_k(t)dt.$$

Taking Fourier transforms of equation (3.11) gives

$$-i\omega\widetilde{\eta}_k(\omega) = \sum_{l=E,I} J_{kl}\widetilde{\eta}_l(\omega) + b_k(\mathbf{x}^*)\widetilde{\xi}_k(\omega). \tag{3.12}$$

This can be rearranged to give

$$\widetilde{\eta}_k(\omega) = \sum_{l=E,I} \Phi^{-1}_{kl}(\omega)b_l(\mathbf{x}^*)\widetilde{\xi}_l(\omega), \quad \Phi_{kl}(\omega) = -i\omega\delta_{k,l} - J_{kl}. \tag{3.13}$$

The Fourier transform of the white noise process $\xi_k(t)$ has the correlation function

$$\langle \widetilde{\xi}_k(\omega)\widetilde{\xi}_l(\omega) \rangle = 2\pi\delta_{k,l}\delta(\omega+\omega'). \tag{3.14}$$

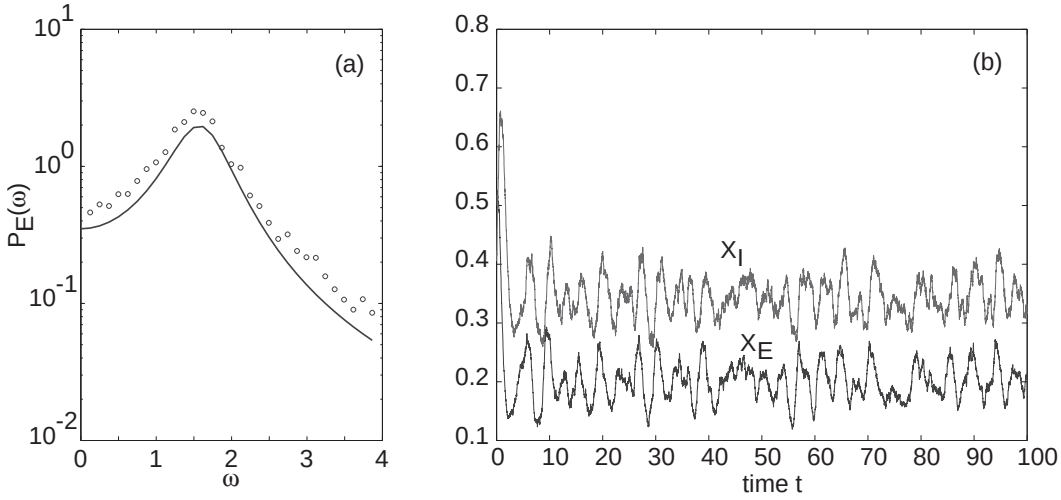

Figure 3: Noise-amplification of subthreshold oscillations in an E-I network. (a) Power spectrum of excitatory fluctuations (solid curve) obtained by Fourier transforming the Langevin equation (3.11). Data points are from stochastic simulations of full master equation with $N = 1000$, averaged over 100 samples. (b) Sample trajectories obtained from stochastic simulations of full master equation with $N = 100$. Same weight parameter values as Fig. 2 with $h_E = 0$, $h_I = -2$.

The power spectrum is defined according to

$$2\pi\delta(0)P_k(\omega) = \langle|\widetilde{\eta}_k(\omega)|^2\rangle, \tag{3.15}$$

so that equations (3.13) and (3.14) give

$$P_k(\omega) = \sum_{l=E.I} |\Phi^{-1}_{kl}(\omega)|^2 B_l(\mathbf{x}^*), \tag{3.16}$$

with $B_l(\mathbf{x}^*) = b_l(\mathbf{x}^*)^2$. The right–hand side can be evaluated explicitly to yield

$$P_k(\omega) = \frac{\beta_k + \gamma_k\omega^2}{|D(\omega)|^2} \tag{3.17}$$

with $D(\omega) = \mathrm{Det}\,\Phi(\omega) = -\omega^2 + i\omega\mathrm{Tr}\,\mathbf{J} + \mathrm{Det}\,\mathbf{J}$ and

$$\beta_E = J^2_{22}B_E(\mathbf{x}^*) + J^2_{12}B_I(\mathbf{x}^*), \quad \gamma_E = B_E(\mathbf{x}^*) \tag{3.18}$$

$$\beta_I = J^2_{21}B_E(\mathbf{x}^*) + J^2_{11}B_I(\mathbf{x}^*), \quad \gamma_I = B_I(\mathbf{x}^*). \tag{3.19}$$

Finally, evaluating the denominator and using the stability conditions $\mathrm{Tr}\,\mathbf{J} < 0$, $\mathrm{Det}\,\mathbf{J} > 0$, we have [47]

$$P_k(\omega) = \frac{\beta_k + \gamma_k\omega^2}{(\omega^2 - \Omega_0^2)^2 + \Gamma^2\omega^2} \tag{3.20}$$

where we have set $\Gamma = \mathrm{Tr}\,\mathbf{J}$ and $\Omega_0^2 = \mathrm{Det}\,\mathbf{J}$. In Fig. 3, we compare our analytical calculation of the spectrum for subthreshold oscillations in an E-I network with direct simulations of the full master equation (2.1). We choose a point in parameter space that lies just above the upper Hopf curve in Fig. 2 by taking $h_E = 0, h_I = -2$. The only fixed point is a stable focus. It can be seen in Fig. 3(a) that the spectrum exhibits a strong peak at a frequency $\omega \approx 1.5$, which is close to the Hopf frequency of limit cycle oscillations generated by crossing the nearby Hopf bifurcation boundary by decreasing the inhibitory input h_I. Sample trajectories for the stochastic variables $X_E(t)$ and $X_I(t)$ also indicate oscillatory–like behavior, see Fig. 3(b).

4 Stochastic phase reduction

Let us now suppose that the E-I system introduced in section 3 is operating in a parameter regime where the mean–field equations (3.1) support a stable limit cycle, as illustrated in Fig. 4. It is then possible to extend the spectral analysis of the Langevin equation (2.12) using Floquet theory [5]. However, in order to investigate the effects of intrinsic noise on noise–induced synchronization (see section 5), we will proceed by carrying out a stochastic phase reduction of the Langevin equation (2.12). For the moment we set the extrinsic noise source to zero ($\sigma = 0$). The phase reduction method [37, 20] requires the application of standard rules of calculus. Therefore, it is first necessary to convert the Ito SDE (2.12) to a Stratonovich SDE [24, 19]:

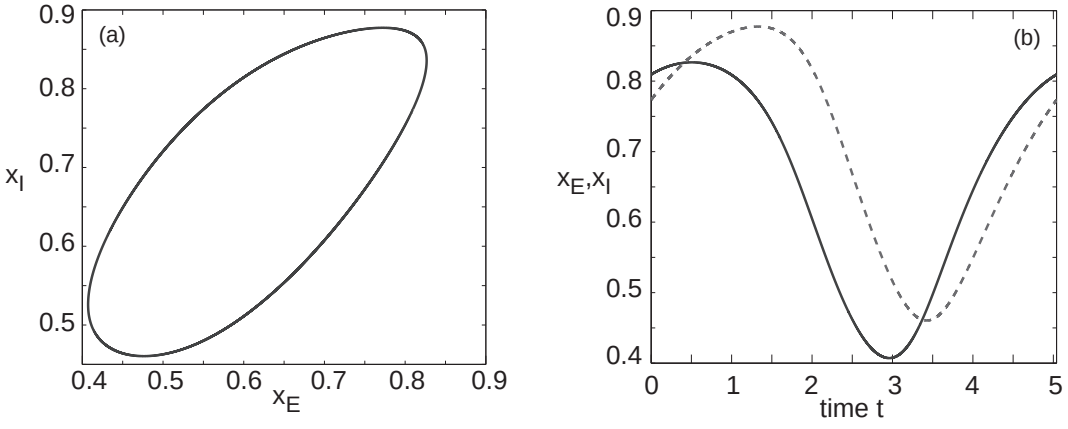

Figure 4: Limit cycle in a deterministic E-I network with parameters $w_{EE} = 11.5, w_{IE} = -w_{EI} = 10$, $w_{II} = -2$, $h_E = 0$ and $h_I = -4$. Also $F(u) = 1/(1 + \mathrm{e}^{-u})$. (a) Limit cycle in the (x_E, x_I)–plane. (b) Trajectories along the limit cycle for $x_E(t)$ (solid curve) and $x_I(t)$ (dashed curve).

$$dX_k = \left[A_k(\mathbf{X}) - \frac{\epsilon^2}{2} b_k(\mathbf{X}) \frac{\partial b_k(\mathbf{X})}{\partial X_k} \right] dt + \epsilon b_k(\mathbf{X}) dW_k(t), k = E, I. \tag{4.1}$$

Denote the stable limit cycle solution of the corresponding deterministic system ($\epsilon = 0$) by $\mathbf{x}^*(\theta)$ where $\theta(t) = \omega t$ and ω is the natural frequency of the limit cycle oscillator. We can extend the notion of phase into a neighborhood $\mathcal{M} \subset \mathbb{R}^2$ of the limit cycle, that is, there exists an isochronal mapping $\Psi : \mathcal{M} \to [-\pi, \pi)$ with $\theta = \Psi(\mathbf{x})$. This allows us to define a stochastic phase variable according to $\Theta(t) = \Psi(\mathbf{X}(t)) \in [-\pi, \pi)$ when the ϵ–dependent perturbations are included. The phase reduction method then leads to the following Stratonovich Langevin equation for the phase dynamics [64, 49, 65]:

$$d\Theta = \omega + \sum_{k=I,E} Z_k(\Theta) \left[-\frac{\epsilon^2}{2} b_k(\Theta) \partial b_k(\Theta) dt + \epsilon b_k(\Theta) dW_k(t) \right]. \tag{4.2}$$

Here $Z_k(\theta)$ is the kth component of the infinitesimal phase resetting curve (PRC) defined as

$$Z_k(\theta) = \left. \frac{\partial \Psi(\mathbf{x})}{\partial x_k} \right|_{\mathbf{x}=\mathbf{x}^*(\theta)} \tag{4.3}$$

with $\sum_{k=E,I} Z_k(\theta) A_k(\mathbf{x}^*(\theta)) = \omega$. All the terms multiplying $Z_k(\theta)$ are evaluated on the limit cycle so that

$$b_k(\theta)) = b_k(\mathbf{x}^*(\theta)), \quad \partial b_k(\theta) = \left. \frac{\partial b_k(\mathbf{x})}{\partial x_k} \right|_{\mathbf{x}_k=\mathbf{x}_k^*(\theta)}.$$

It can be shown that the PRC is the unique 2π–periodic solution of the adjoint linear equation [20]

$$\frac{dZ_k}{dt} = -\sum_{l=E,I} A_{lk}(\mathbf{x}^*(t)) Z_l(t), \tag{4.4}$$

where $A_{lk} = \partial A_l / \partial x_k$, which is supplemented by the normalization condition $\sum_k Z_k(t) dx_k^*/dt = 1$. The PRC can thus be evaluated numerically by solving the adjoint equation backwards in time. (This exploits the fact that all non-zero Floquet exponents of solutions to the adjoint equation are positive). An example of the PRC for an oscillating E-I network is shown in Fig. 4, which establishes that both components of the PRC are type II, that is, they take both positive and negative values.

We can use the Langevin equation (4.2) to analyze the effects of intrinsic noise on limit cycle oscillations. Following along analogous lines to the study of single neurons [19], we consider the distribution of first passage times T for the system to complete one cycle, that is, $\Theta(T) = 2\pi$ given that $\Theta(0) = 0$. In order to solve the first passage time problem, we first convert equation (4.2) into an Ito SDE [24]:

$$d\Theta = \mathcal{A}_0(\Theta) dt + \epsilon \sum_{k=E,I} Z_k(\Theta) b_k(\Theta) dW_k(t), \tag{4.5}$$

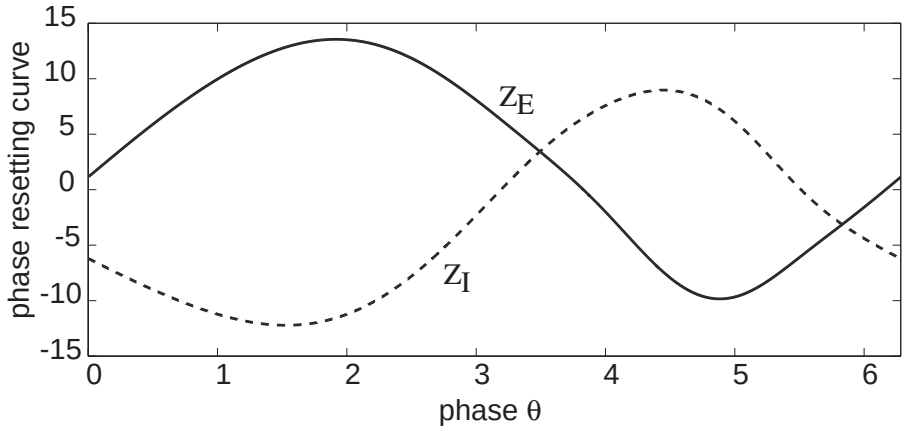

Figure 5: Components Z_E and Z_I of phase resetting curve for an E-I network supporting limit cycle oscillations in the deterministic limit. Same network parameter values as Fig. 4.

where

$$\mathcal{A}_0(\theta) = \omega - \frac{\epsilon^2}{2}\sum_{k=E,I} Z_k(\theta)b_k(\theta)\partial b_k(\theta) + \frac{\epsilon^2}{2}\sum_{k=E,I} Z_k(\theta)b_k(\theta)(Z_k(\theta)b_k(\theta))'. \tag{4.6}$$

Corresponding to the SDE (4.5) is the Fokker–Planck equation for the 2π–periodic probability density function $P(\theta, t)$:

$$\frac{\partial P}{\partial t} = -\frac{\partial}{\partial \theta}[\mathcal{A}_0(\theta)P(\theta,t)] + \frac{1}{2}\frac{\partial^2}{\partial \theta^2}[\mathcal{B}_0(\theta)P(\theta,t)], \tag{4.7}$$

where

$$\mathcal{B}_0(\theta) = \epsilon^2 \sum_{k=E,I} [Z_k(\theta)b_k(\theta)]^2. \tag{4.8}$$

In order to formulate the first passage time problem, we replace the periodic boundary conditions by a reflecting boundary at $\theta = 0$ and an absorbing boundary at $\theta = 2\pi$. This exploits the fact that for sufficiently small ϵ the probability of crossing $\theta = 0$ from above can be neglected. Introducing the probability flux

$$J(\theta,t) = \mathcal{A}_0(\theta)P(\theta,t) - \frac{1}{2}\frac{\partial}{\partial\theta}[\mathcal{B}_0(\theta)P(\theta,t)], \tag{4.9}$$

the boundary conditions take the form

$$J(0,t) = 0, \quad P(2\pi,t) = 0 \tag{4.10}$$

Let $T(\theta)$ denote the first passage time to reach 2π given that the system started at $\theta \in [0, 2\pi)$. Then

$$\text{Prob}(T(\theta) \geq t) = \int_0^{2\pi} P(\theta', t|\theta, 0))d\theta' \equiv \mathcal{G}(\theta, t), \tag{4.11}$$

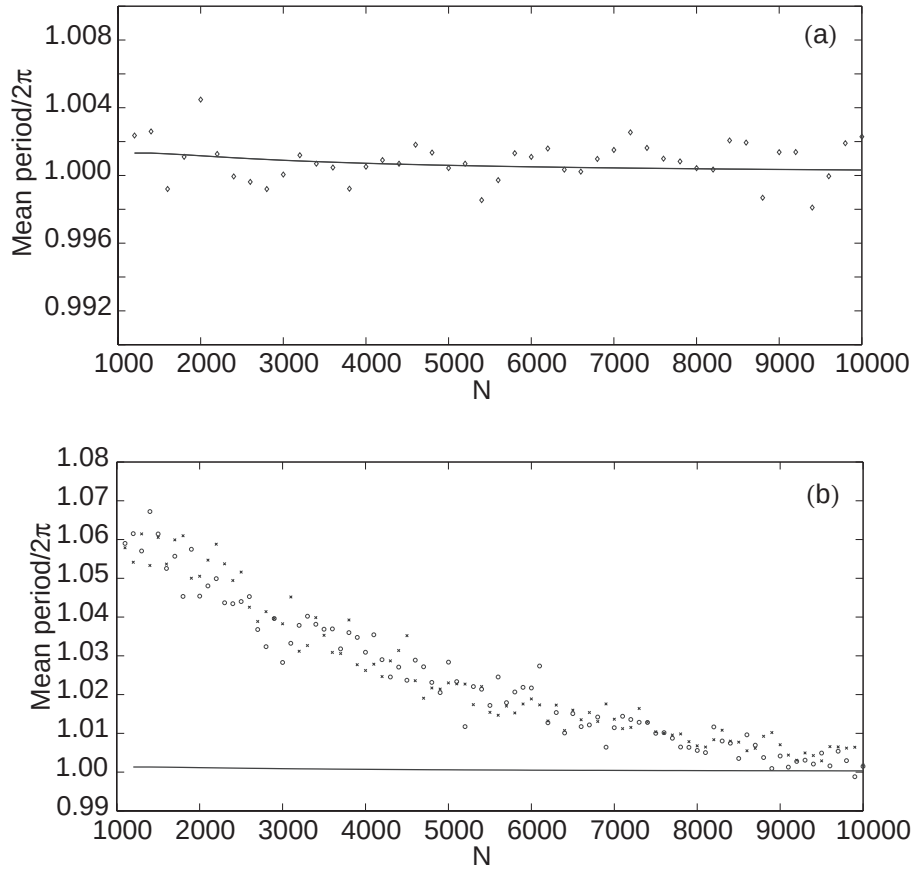

Figure 6: Mean period of the stochastic E-I network as a function of system size N. Same network parameters as Fig. 4. (a) Comparison of the MFPT (solid line) with simulations of the phase-reduced Langevin equation (diamonds). (b) Comparison of the MFPT (solid line) with simulations of the full master equation (circles) and simulations of the planar Langevin equation (crosses). Each data point is the average of 10^5 cycles. The master equation is simulated using the Gillespie algorithm with τ–leaping [16, 17], whereas the Langevin equations are simulated using the Euler–Maruyama algorithm [24] applied to the Ito version.

where the initial condition for P is now made explicit. Given the distribution $\mathcal{G}(\theta,t)$, the moments of the first passage time $T(\theta)$ can be calculated according to [24]

$$T_n(\theta) \equiv \langle T^n(\theta)\rangle = n\int_0^\infty t^{n-1}\mathcal{G}(\theta,t)dt. \tag{4.12}$$

Moreover, from the corresponding backwards Fokker–Planck equation it can be shown that the

moments satisfy the iterative set of equations [24]

$$-nT_{n-1}(\theta) = \mathcal{A}_0(\theta)T_n'(\theta) + \frac{1}{2}\mathcal{B}_0(\theta)T_n''(\theta), \quad n \geq 0 \tag{4.13}$$

with boundary conditions $T_n'(0) = 0, T_n(2\pi) = 0$ and $T_0 \equiv 1$.

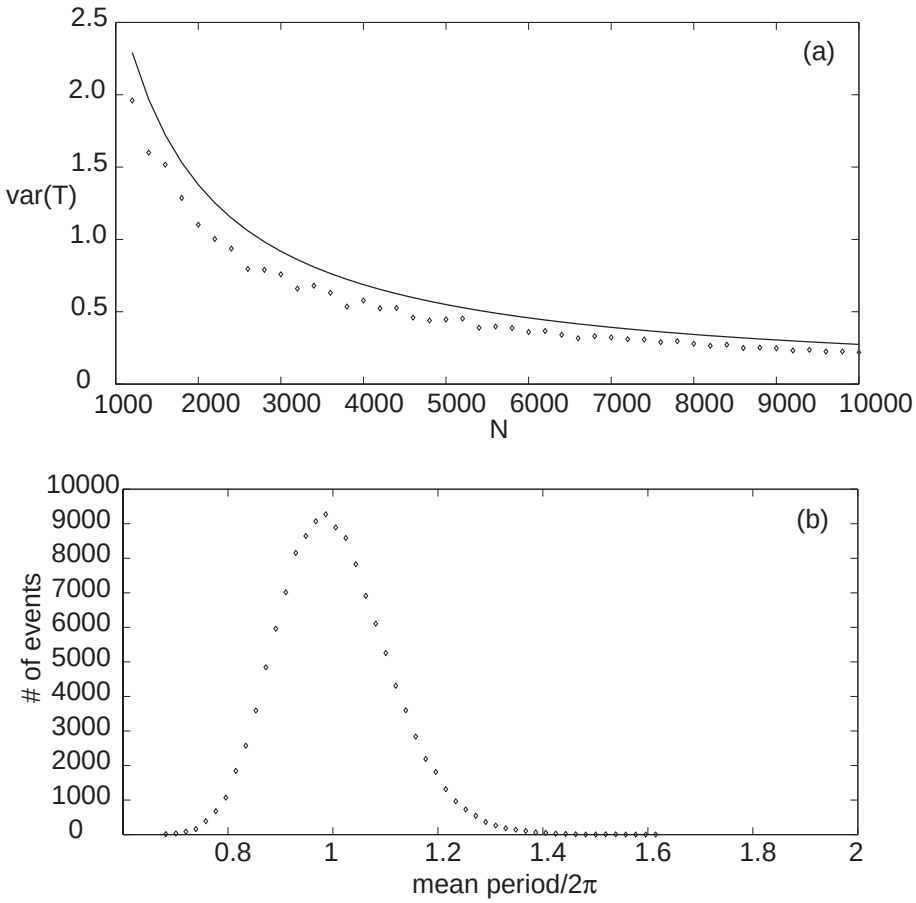

Figure 7: (a) Variance var(T) of the period of oscillations as a function of system size N. The solid line is based on the second moments of the first passage time distribution and diamonds are from simulations of the phase-reduced Langevin equation. (b) Histogram of period of oscillations for 10^5 cycles and $N = 5000$.

Of particular interest from the viewpoint of limit cycle oscillations are the mean period $T_1(0)$ and variance $T_2(0) - T_1(0)^2$. These are shown in Figs. 6 and 7. Looking at the figure for the mean period, one sees that there is reasonable agreement between stochastic simulations and our analytical calculations for larger N (i.e. smaller intrinsic noise). However, for smaller N, although there is still reasonable agreement between the simulations of the phase-reduced

Langevin equation (4.5) and the analysis based on the MFPT, there are discrepancies when comparing with simulations of the full master equation or the corresponding planar Langevin equation (4.1). This is partly due to the difficulty in numerically evaluating the asymptotic phase of a point not on the limit cycle. In particular, the high magnitude of the phase response curves Z_E, Z_I (see Fig. 5) indicates that small perturbations off the limit cycle cause relatively large changes in phase. Thus, for smaller values of N, intrinsic noise fluctuations induce larger perturbations off the limit cycle such that the phase reduction method becomes less accurate. This is because the phase response curve does not apply exactly unless the system has relaxed back to the limit cycle - that is, the approximation

$$\nabla_{\mathbf{x}}\theta \approx \nabla_{\mathbf{x}}\theta|_{\mathbf{x}=\mathbf{x}^*(\theta)} \equiv \mathbf{Z}$$

can lead to significant errors [30]. In addition, each of the curves generated by our stochastic simulations are noisy despite averaging over many trials. This is due to the relatively high variance of the oscillation period (see Fig. 7(a)). This is also shown by the relatively broad distribution of oscillation periods (see Fig. 7(b)).

5 Noise–induced synchronization

Now suppose that there exists an ensemble of $\mathcal{N}$ identical, uncoupled $E-I$ systems labelled by μ, each with its own source of intrinsic noise and driven by a common source of extrinsic noise. Thus, each $E-I$ network evolves according to a Langevin equation of the form (2.16):

$$dX_k^{(\mu)} = A_k(\mathbf{X}^{(\mu)})dt + \epsilon b_k(\mathbf{X}^{(\mu)})dW_k^{(\mu)}(t) + \sigma a_k(\mathbf{X}^{(\mu)})dW(t). \tag{5.1}$$

For the moment, we assume that the strength of the extrinsic noise is the same for both excitatory and inhibitory populations by taking $\chi_E = \chi_I = 1/2$ in equations (2.14) and (2.17). Note that we associate an independent set of Wiener processes $W_k^{(\mu)}, k = E, I$ with each $E-I$ network but take the extrinsic noise to be common to all populations. Thus,

$$\langle dW_k^{(\mu)}(t)dW_l^{(\nu)}(t)\rangle = \delta_{k,l}\delta_{\mu,\nu}dt \tag{5.2}$$

$$\langle dW_k^{(\mu)}(t)dW(t)\rangle = 0 \tag{5.3}$$

$$\langle dW(t)dW(t)\rangle = dt. \tag{5.4}$$

Carrying out the phase reduction procedure along identical lines to that of section 4, noting that the extrinsic noise is already in Stratonovich form, we obtain the following set of Stratonovich SDEs for the stochastic phase variables $\Theta^{(\mu)}, \mu = 1, \ldots, \mathcal{N}$:

$$d\Theta^{(\mu)} = \left[\omega - \frac{\epsilon^2}{2}\Omega(\Theta^{(\mu)})\right]dt + \epsilon \sum_{k=E,I} \beta_k(\Theta^{(\mu)})dW_k^{(\mu)}(t) + \sigma\alpha(\Theta^{(\mu)})dW(t), \tag{5.5}$$

where

$$\beta_k(\theta) = Z_k(\theta)b_k(\theta), \quad \Omega(\theta) = \sum_{k=E,I} Z_k(\theta)b_k(\theta)\partial b_k(\theta),, \quad \alpha(\theta) = \sum_{k=E,I} Z_k(\theta)a_k(\theta). \tag{5.6}$$

We now convert equation (5.5) to an Ito SDE of the form

$$d\Theta^{(\mu)} = \mathcal{A}^{(\mu)}(\mathbf{\Theta})dt + d\zeta^{(\mu)}(\mathbf{\Theta}, t), \tag{5.7}$$

where $\{\zeta^{(\mu)}(\mathbf{\Theta}, t)\}$ are correlated Wiener processes with $\mathbf{\Theta} = (\Theta^{(1)}, \ldots, \Theta^{(\mathcal{N})})$. That is,

$$d\zeta^{(\mu)}(\mathbf{\Theta}, t) = \epsilon \sum_{k=E,I} \beta_k(\Theta^{(\mu)})dW_k^{(\mu)}(t) + \sigma\alpha(\Theta^{(\mu)})dW(t), \tag{5.8}$$

with $\langle d\zeta^{(\mu)}(\mathbf{\Theta}, t)\rangle = 0$ and $\langle d\zeta^{(\mu)}(\mathbf{\Theta}, t)d\zeta^{(\nu)}(\mathbf{\Theta}, t)\rangle = C^{(\mu\nu)}(\mathbf{\Theta})dt$, where $C^{(\mu\nu)}(\boldsymbol{\theta})$ is the equal–time correlation matrix

$$C^{(\mu\nu)}(\boldsymbol{\theta}) = \sigma^2\alpha(\theta^{(\mu)})\alpha(\theta^{(\nu)}) + \epsilon^2 \sum_{k=E,I} \beta_k(\theta^{(\mu)})\beta_k(\theta^{(\nu)})\delta_{\mu,\nu}. \tag{5.9}$$

The drift term $\mathcal{A}^{(\mu)}(\boldsymbol{\theta})$ is given by (cf. equation (4.6))

$$\mathcal{A}^{(\mu)}(\boldsymbol{\theta}) = \omega - \frac{\epsilon^2}{2}\Omega(\theta^{(\mu)}) + \frac{1}{4}\mathcal{B}'(\theta^{(\mu)}) \tag{5.10}$$

with Ω given by equation (5.6) and

$$\mathcal{B}(\theta^{(\mu)}) \equiv C^{(\mu\mu)}(\boldsymbol{\theta}) = \sigma^2[\alpha(\theta^{(\mu)})]^2 + \epsilon^2 \sum_{k=E,I} [\beta_k(\theta^{(\mu)})]^2. \tag{5.11}$$

It follows that the ensemble is described by a multivariate Fokker–Planck equation of the form

$$\frac{\partial P(\boldsymbol{\theta}, t)}{\partial t} = -\sum_{\mu=1}^{\mathcal{N}} \frac{\partial}{\partial\theta^\mu}[\mathcal{A}^{(\mu)}(\boldsymbol{\theta})P(\boldsymbol{\theta}, t)] + \frac{1}{2}\sum_{\mu,\nu=1}^{\mathcal{N}} \frac{\partial^2}{\partial\theta^\mu\partial\theta^\nu}[C^{(\mu\nu)}(\boldsymbol{\theta})P(\boldsymbol{\theta}, t)]. \tag{5.12}$$

Having obtained the FP equation (5.12), we now carry out an averaging procedure along similar lines to Nakao *et. al.* [49]. The one major difference is that here the uncorrelated noise arises from intrinsic fluctuations within each neural population rather than as an additional extrinsic noise source. Consequently, there is an additional contribution to the drift term $\mathcal{A}^{(\mu)}$ arising from the fact that the uncorrelated intrinsic noise term appearing in the neural Langevin equation (5.1) is Ito rather than Stratonovich. Introduce the slow phase variables $\boldsymbol{\psi} = (\psi^{(1)}, \ldots, \psi^{(\mathcal{N})})$ according to $\theta^\mu = \omega t + \psi^\mu$ and set $Q(\boldsymbol{\psi}, t) = P(\{\omega t + \theta^{(\mu)}\}, t)$ so that

$$\frac{\partial Q}{\partial t} = \frac{\partial P}{\partial t} + \omega\sum_\mu \frac{\partial P}{\partial\theta^{(\mu)}}.$$

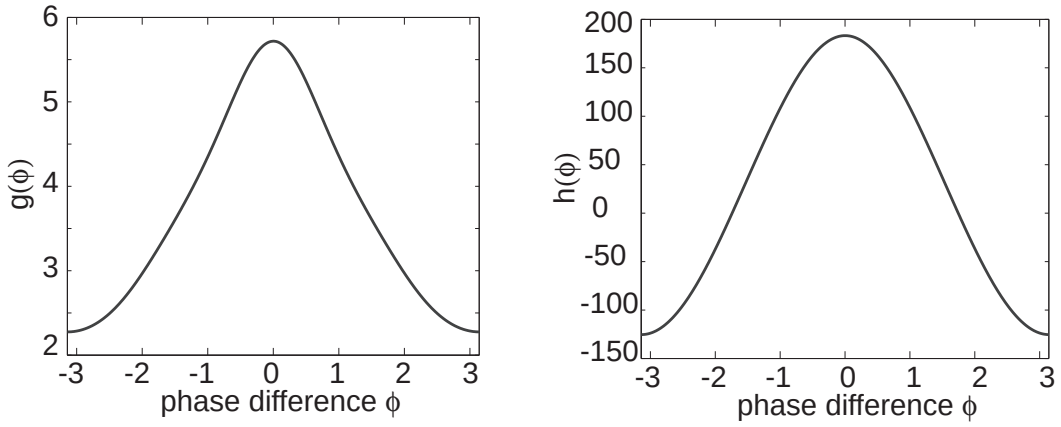

Figure 8: Plot of periodic functions g and h for an E-I limit cycle oscillator with symmetric stochastic drive to excitatory and inhibitory populations ($\chi_E = \chi_I = 1/2$). Same network parameters as Fig. 4.

For sufficiently small ϵ and σ, Q is a slowly varying function of time so that we can average the Fokker-Planck equation for Q over one cycle of length $\tau = 2\pi/\omega$. In particular,

$$\begin{aligned}\langle \mathcal{A}^{(\mu)}(\boldsymbol{\theta})\rangle_\tau &= \frac{1}{\tau}\int_t^{t+\tau}\left[\omega - \frac{\epsilon^2}{2}\Omega(\psi^{(\mu)}+\omega t') + \frac{1}{4}\mathcal{B}'(\psi^{(\mu)}+\omega t')\right]dt' \\ &= \omega - \frac{\epsilon^2}{2}\overline{\Omega} \end{aligned} \tag{5.13}$$

with

$$\overline{\Omega} = \frac{1}{2\pi}\int_0^{2\pi}\Omega(\theta)d\theta. \tag{5.14}$$

Similarly,

$$\begin{aligned}\langle C^{(\mu\nu)}(\boldsymbol{\theta})\rangle_\tau &= \frac{1}{\tau}\int_t^{t+\tau}\left[\sigma^2\alpha(\psi^{(\mu)}+\omega t')\alpha(\psi^{(\nu)}+\omega t') + \epsilon^2\sum_{k=E,I}\beta_k(\psi^{(\mu)}+\omega t')\beta_k(\psi^{(\nu)}+\omega t')\delta_{\mu,\nu}\right]dt' \\ &= \sigma^2 g(\psi^{(\mu)}-\psi^{(\nu)}) + \epsilon^2 h(0)\delta_{\mu,\nu} \\ &= \overline{C}^{(\mu\nu)}(\boldsymbol{\psi}) \end{aligned} \tag{5.15}$$

where

$$g(\psi) = \frac{1}{2\pi}\int_{-\pi}^{\pi}\alpha(\theta')\alpha(\theta'+\psi)d\theta' \tag{5.16}$$

$$h(\psi) = \frac{1}{2\pi}\int_{-\pi}^{\pi}\sum_{k=E,I}\beta_k(\theta')\beta_k(\theta'+\psi)d\theta' \tag{5.17}$$

The averaged FP equation for Q is thus (see also Ref. [49])

$$\frac{\partial Q(\boldsymbol{\psi},t)}{\partial t} = \frac{\epsilon^2}{2}\overline{\Omega}\sum_{\mu=1}^{\mathcal{N}}\frac{\partial}{\partial\psi^\mu}Q(\boldsymbol{\psi},t) + \frac{1}{2}\sum_{\mu,\nu=1}^{\mathcal{N}}\frac{\partial^2}{\partial\psi^\mu\partial\psi^\nu}[\overline{C}^{(\mu\nu)}(\boldsymbol{\psi})Q(\boldsymbol{\psi},t)]. \tag{5.18}$$

An example plot of the periodic functions $g(\psi), h(\psi)$ is given in Fig. 8.

Following Nakao *et. al.*, we can investigate noise–induced synchronization by focussing on the phase difference between two $E-I$ networks. Setting $\mathcal{N}=2$ in equation (5.18) gives

$$\begin{aligned}\frac{\partial Q}{\partial t} &= \frac{\epsilon^2}{2}\overline{\Omega}\left[\frac{\partial Q}{\partial\psi^{(1}} + \frac{\partial Q}{\partial\psi^{(2)}}\right] + \frac{1}{2}\left[\sigma^2 g(0) + \epsilon^2 h(0)\right]\left[\left(\frac{\partial}{\partial\psi^{(1)}}\right)^2 + \left(\frac{\partial}{\partial\psi^{(2)}}\right)^2\right]Q \\ &\quad + \frac{\partial^2}{\partial\psi^{(1)}\partial\psi^{(2)}}[\sigma^2 g(\psi^{(1)}-\psi^{(2)})Q].\end{aligned} \tag{5.19}$$

Performing the change of variables

$$\psi = (\psi^{(1)}+\psi^{(1)})/2, \quad \phi = \psi^{(1)} - \psi^{(1)} \tag{5.20}$$

and writing $Q(\psi^{(1)},\psi^{(2)},t) = \Psi(\psi,t)\Phi(\phi,t)$ we obtain the pair of PDEs

$$\frac{\partial\Psi}{\partial t} = \frac{\epsilon^2}{2}\overline{\Omega}\frac{\partial\Psi}{\partial\psi} + \frac{1}{4}\left[\sigma^2(g(0)+g(\phi)) + \epsilon^2 h(0)\right]\frac{\partial^2\Psi}{\partial\psi^2} \tag{5.21}$$

and

$$\frac{\partial\Phi}{\partial t} = \frac{\partial^2}{\partial\phi^2}\left[\sigma^2(g(0)-g(\phi)) + \epsilon^2 h(0)\right]\Phi. \tag{5.22}$$

These have the steady–state solution

$$\Psi_0(\psi) = \frac{1}{2\pi}, \quad \Phi_0(\phi) = \frac{\Gamma_0}{\sigma^2(g(0)-g(\phi)) + \epsilon^2 h(0)}, \tag{5.23}$$

where Γ_0 is a normalization constant.

The distribution $\Phi_0(\phi)$ allows us to characterize the effects of uncorrelated intrinsic noise on noise–induced synchronization. In the absence of a common extrinsic noise source ($\sigma=0$) and $\epsilon>0$, $\Phi_0(\phi)$ is a uniform distribution, which means that the oscillators are completely desynchronized. On the other hand, in the thermodynamic limit $\epsilon = N^{-1/2}\to 0$ and $\sigma>0$, the distribution Φ_0 diverges at $\theta=0$, so that the phase difference between any pair of E-I limit cycle oscillators accumulates at zero, signifying complete synchronization induced by a common extrinsic noise signal. As ϵ increases from zero, the intrinsic noise arising from finite–size effects becomes more important, resulting in the broadening of the distribution $\Phi_0(\phi)$. Note that in the given parameter regime, the periodic function g is unimodal with $g(0)\geq g(\phi)$ (see Fig. 8), so that Φ_0 is also unimodal with a peak at $\phi=0$. The width and height of the peak depend

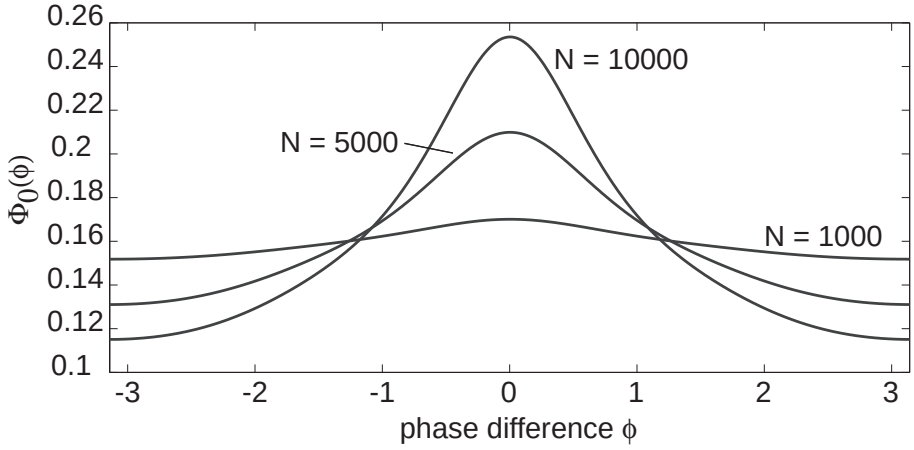

Figure 9: Probability distribution of the phase difference between a pair of E-I oscillators as a function of system size N for fixed extrinsic noise $\sigma = 0.08$ with g, h given by Fig. 8. Increasing N causes the curve to have a much sharper peak and much more synchronization.

directly on the relative strengths of the intrinsic noise ϵ and extrinsic noise σ. This is illustrated in Figs. 9 and 10. The latter also shows that there is good agreement between our analytical calculations and numerical simulations of the phase–reduced Langevin equations. We simulated the phase oscillators by using an Euler-Maruyama scheme on the Ito Langevin equation (5.7). A large number $\mathcal{M} \approx O(10^2)$ of oscillators were simulated up to a large time T (obtained by trial and error), by which time their pairwise phase differences had reached a steady state. As we were comparing pairwise phase differences each simulation gave us $\frac{1}{2}\mathcal{M}(\mathcal{M}-1)$ data points and we averaged over many simulations to obtain 10^6 data points for each diagram in Figure 10. These were then placed into 50 bins along $[-\pi, \pi)$ and normalised. Also shown in Fig. 10(b) are data points obtained from simulations of the full planar Langevin equations. Here computations were much slower so we only averaged over relatively few trials and thus the data is more noisy. Nevertheless a reasonable fit with the analytical distribution can still be seen.

Nakao *et. al.* have previously shown that in the case of Stuart-Landau or Fitzhugh–Nagumo limit cycle oscillators with both uncorrelated and correlated extrinsic noise sources, parameter regimes can be found where the periodic function g has multiple peaks [49]. This can occur when higher harmonics of the phase resetting curve become dominant or when the common noise source is multiplicative. The presence of multiple peaks in g results in an ensemble of oscillators forming clustered states. Moreover, there are intermittent transitions between the clustered states induced by the uncorrelated noise. In the case of stochastic E-I limit cycle oscillators, we were unable to find a parameter regime where g develops multiple peaks when the

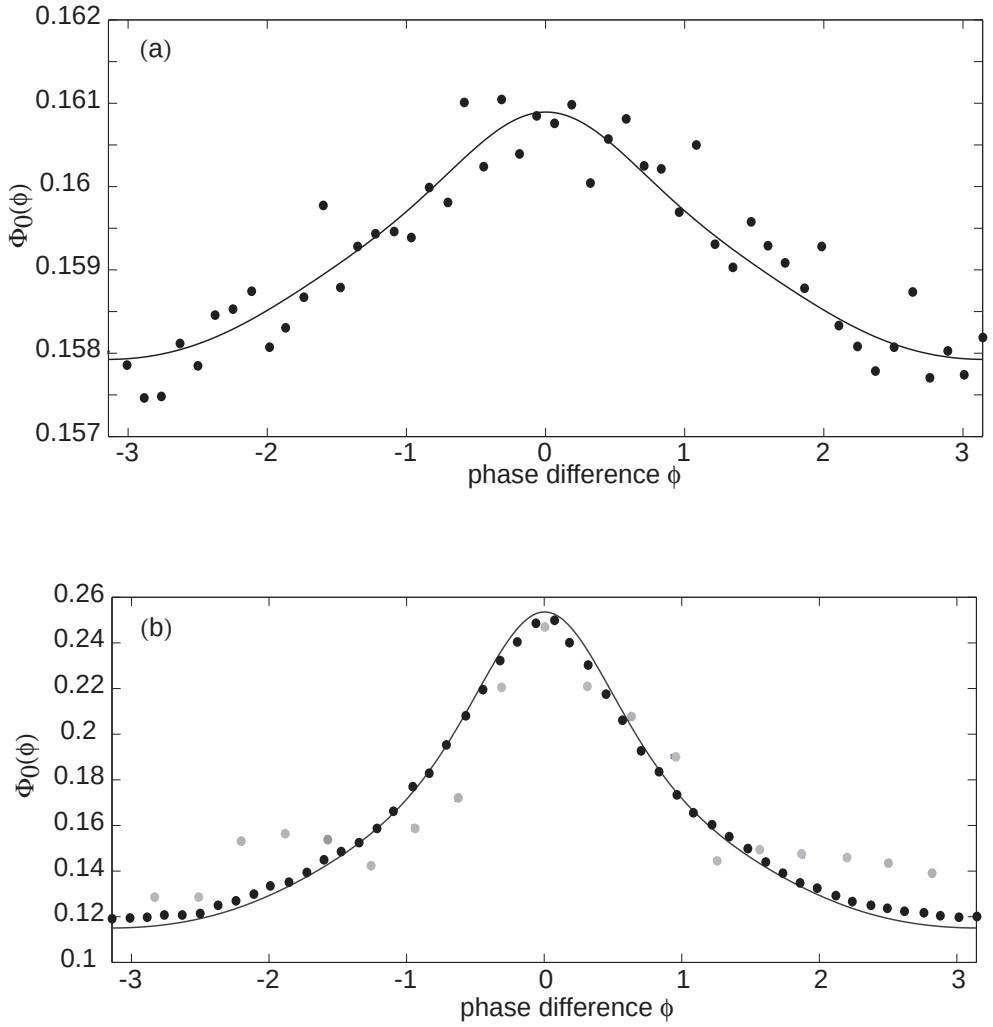

Figure 10: Probability distribution of the phase difference between a pair of E-I oscillators as a function of extrinsic noise strength σ with g, h given by Fig. 8. Solid curves are based on analytical calculations, whereas black (gray) filled circles correspond to stochastic simulations of the phase–reduced (planar) Langevin equations. (a) $N = 10^5$, $\sigma = 0.01$. The curve is very flat, showing little synchronization. (b) $N = 10^5$, $\sigma = 0.08$. Increasing σ causes the curve to have a much sharper peak and much more synchronization.

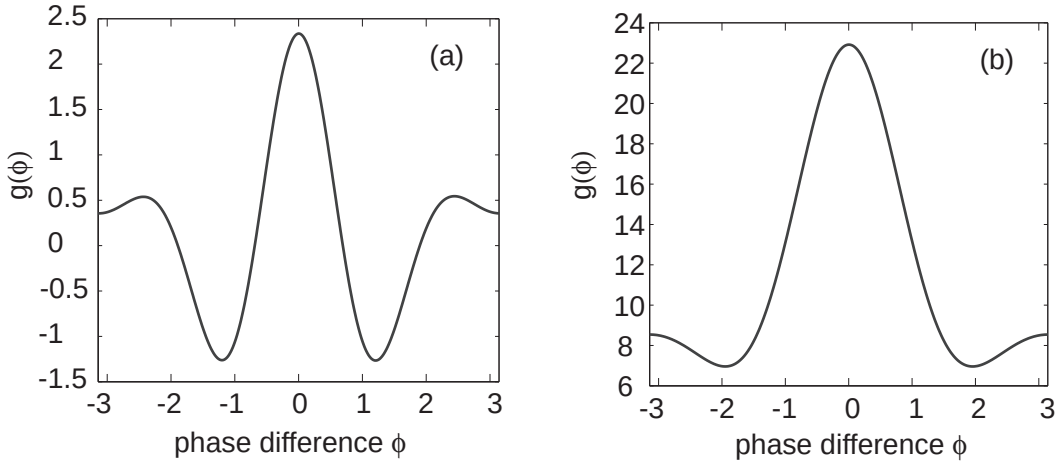

Figure 11: Periodic function g with multiple peaks when there is an asymmetry in the common extrinsic noise source to the excitatory and inhibitory populations. Other network parameters are as in Fig. 4. (a) $\chi_E = 1/8, \chi = 7/8$ so that common stochastic drive is mainly to the inhibitory population. (b) $\chi_E = 7/8, \chi = 1/8$ so that common stochastic drive is mainly to the excitatory population.

common extrinsic noise source is the same for both excitatory and inhibitory populations, that is, $\chi_E = \chi_I = 1/2$ in equations (2.14) and (2.17). However, multiple peaks can occur when there is an asymmetry between the excitatory and inhibitory stochastic drives, as illustrated in Fig. 11. The corresponding stationary distribution $\Phi_0(\phi)$ for the phase differences ϕ also develops additional peaks, see Fig.12. When the common stochastic input is mainly presented to the inhibitory population, we find a peak at $\phi = 0$ and smaller peaks at $\phi = \pm 2\pi/3$. Consequently, the ensemble of oscillators tend to cluster in three regions around the limit cycle as shown in the inset of Fig. 12(a). On the other hand, when the stochastic drive is predominantly to the excitatory population, we find a much sharper peak at $\phi = 0$ (compared to the symmetric case) and a small peak at $\phi = \pi$. However, the latter does not contribute significantly to the dynamics, so that the oscillators are strongly synchronized.

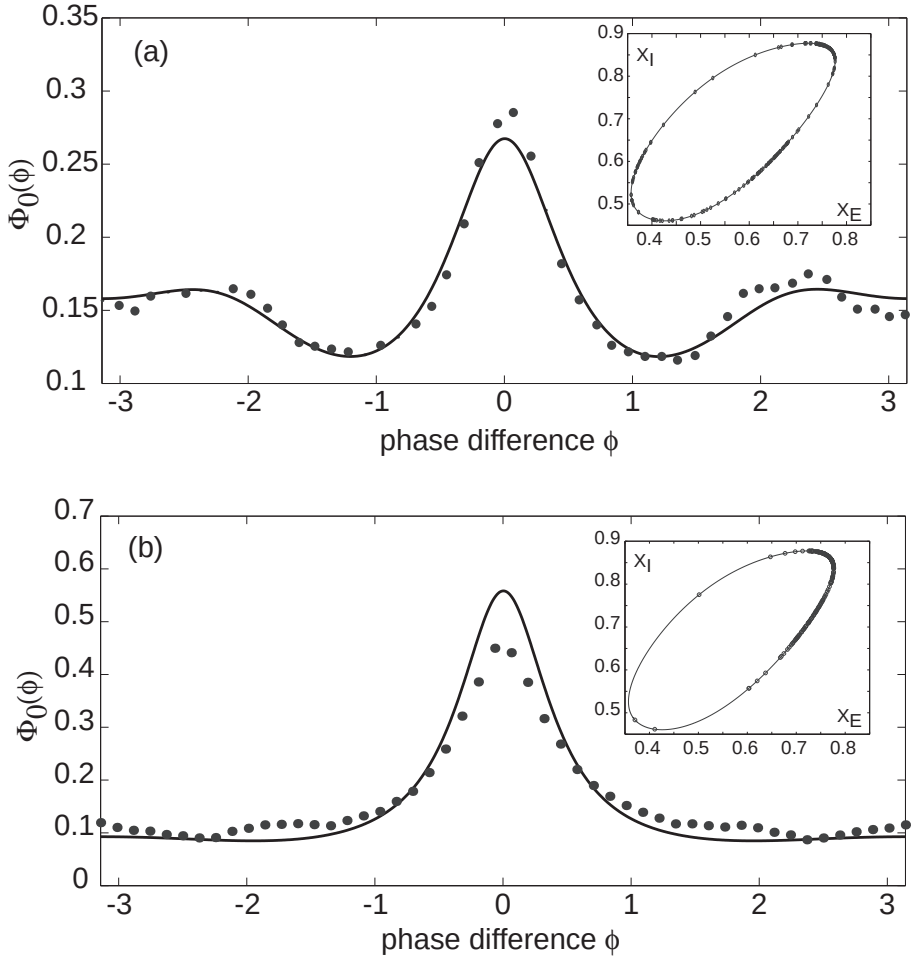

Figure 12: Probability distribution of the phase difference between a pair of E-I oscillators when there is an asymmetry in the common extrinsic noise source to the excitatory and inhibitory populations. Here $N = 10^5$, $\sigma = 0.01$ and other network parameters are as in Fig. 4. Solid curves are based on analytical calculations, whereas black filled circles correspond to stochastic simulations of the phase–reduced Langevin equations. (a) $\chi_E = 1/8, \chi = 7/8$ so that common stochastic drive is mainly to the inhibitory population. (b) $\chi_E = 7/8, \chi = 1/8$ so that common stochastic drive is mainly to the excitatory population. The insets show instantaneous distributions of the oscillators on the limit cycle.

6 Excitatory network with synaptic depression

So far we have applied the stochastic phase reduction method to a two–population model consisting of mutually interacting excitatory and inhibitory populations. This E-I network is one of the simplest population models known to exhibit limit cycle oscillations in the deterministic limit, and forms the basic module in various studies of stimulus–induced oscillations and synchronization in visual cortex [60, 28]. An even simpler population model known to exhibit limit cycle oscillations is a recurrent excitatory network with synaptic depression. For example, Tabak *et. al.* have analyzed Wilson–Cowan mean–field equations representing a recurrent excitatory network with both slow and fast forms of synaptic depression, and used this to model the dynamics of synchronized population bursts in developing chick spinal cord [62, 63]. These burst oscillations are more robust in the presence of an extrinsic noise source or some form of spatial heterogeneity within the network [67, 50]. An excitatory network with synaptic depression and extrinsic noise has also been used to model transitions between cortical Up and Down states [31, 34, 35]. In this section, we consider a stochastic version of an excitatory network with synaptic depression, in which there is both intrinsic noise within the excitatory population and an extrinsic noise source. We carry out a stochastic phase reduction along identical lines to the E-I network and use this to explore the effects of intrinsic noise on noise–induced synchronization.

Let $N(t)$ denote the number of excitatory neurons active at time t, with $P(n,t) = \text{Prob}[N(t) = n]$ evolving according to the master equation (2.1) with $M = 1$:

$$\frac{dP(n,t)}{dt} = T_-(n+1)P(n+1,t) + T_+(n-1,t)P(n-1,t) - [T_-(n) + T_+(n,t)]P(n,t) \quad (6.1)$$

with $P(-1,t) \equiv 0$. The transition rates are taken to be of the Wilson–Cowan form

$$T_{-1}(n) = \alpha n, \quad T_+(n,t) = NF\left(q(t)n/N + I\right), \quad (6.2)$$

where I is an external input, and $q(t)$ is a time–dependent synaptic depression variable. The latter is taken to evolve according to [2, 66, 62, 35]

$$\frac{dq}{dt} = k_+(1-q(t)) - k_-X(t)q(t), \quad X(t) = \frac{N(t)}{N}. \quad (6.3)$$

The depression variable $q(t)$ can be interpreted as a measure of available presynaptic resources at the population level, which are depleted at a rate $k_-X(t)$, which is proportional to the (stochastic) fraction of active neurons $X(t)$, and are recovered at a rate k_+. Note that the master equation (6.1) is non–autonomous due to the dependence of the birth rate T_+ on $q(t)$, with the latter itself coupled to the associated jump Markov process via the depletion rate $\beta X(t)$. Thus equation (6.3) is only defined between jumps, during which q evolves deterministically.

The system defined by equations (6.1)–(6.3) is an example of a so–called stochastic hybrid model based on a piecewise deterministic process. This type of model has recently been applied to genetic networks [71] and to excitable neuronal membranes [52, 12]. In the latter case, the hybrid model provides a mathematical formulation of excitable membranes that incorporates the exact Markovian dynamics of single stochastic ion channels. Moreover, the limit theorems of Kurtz [38] can be adapted to prove convergence of solutions of the hybrid model to solutions of a corresponding Langevin approximation in the limit $N \to \infty$ and finite time, where N is the number of ion channels within the membrane [52, 12].

In the case of our stochastic hybrid model of an excitatory network with synaptic depression, we can heuristically derive a Langevin approximation by first carrying out a Kramers–Moyal expansion of the master equation (6.1). That is, setting $x = n/N$ and treating x as a continuous variable, we Taylor expand the master equation to second order in $1/N$ to obtain the Fokker–Planck equation

$$\frac{\partial P(x,t)}{\partial t} = -\frac{\partial}{\partial x}\left[A(x,q)P(x,t)\right] + \frac{\epsilon^2}{2}\frac{\partial^2}{\partial x^2}\left[B(x,q)P(x,t)\right] \tag{6.4}$$

with $\epsilon = N^{-1/2}$,

$$A(x,q) = F(qx+I) - \alpha x \tag{6.5}$$

and

$$B(x,q) = F(qx+I) + \alpha x. \tag{6.6}$$

The solution to the Fokker–Planck equation (6.4) determines the probability density function for a corresponding stochastic process $X(t)$, which evolves according to the Langevin equation

$$dX = A(X,Q)dt + \epsilon b(X,Q)dW(t). \tag{6.7}$$

with $b(x,q)^2 = B(x,q)$, $W(t)$ an independent Wiener process and, from equation (6.3),

$$dQ = [k_+(1-Q) - k_- XQ]dt. \tag{6.8}$$

Following along similar lines to the $E-I$ network, we can also include an extrinsic noise source by decomposing the drive to the excitatory population as

$$I = h + \frac{\sigma}{\sqrt{F_0}}\hat{\xi}(t), \tag{6.9}$$

where h is a constant input and $\hat{\xi}(t)$ is a white noise term of strength σ. Substituting for I in equation (6.7) and assuming that σ is sufficiently small, we can Taylor expand to first order in σ to give

$$dX = A(X,Q)dt + \epsilon b(X,Q)dW(t) + \sigma a(X,Q)d\widehat{W}(t), \tag{6.10}$$

where $\widehat{W}$ is a second independent Wiener process and

$$a(x,q) = F'(qx+h)/\sqrt{F_0}. \tag{6.11}$$

6.1 Deterministic network

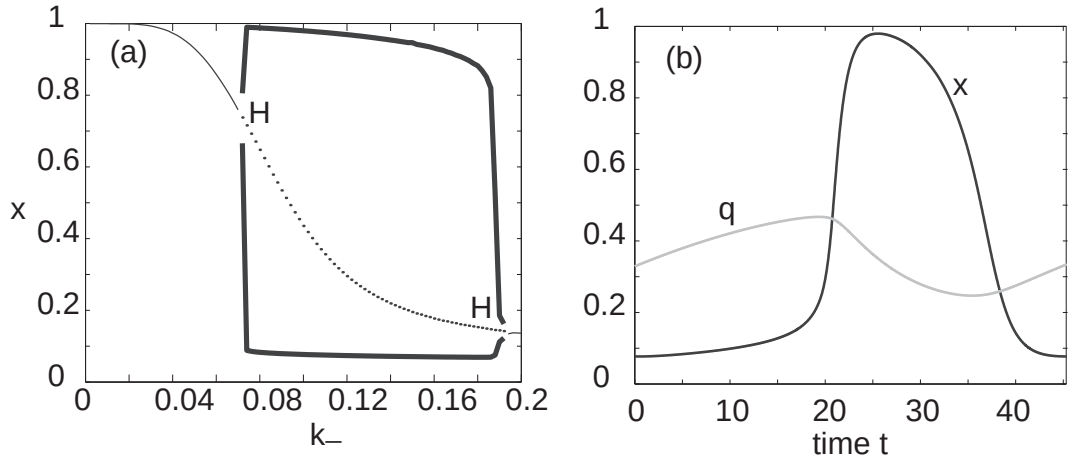

Figure 13: Deterministic excitatory network with synaptic depression. (a) Bifurcation diagram showing solutions as a function of the depletion rate k_-. Stable fixed point (thin solid curve) undergoes a Hop bifurcation at the points H, resulting in an unstable fixed point (dotted curve) and a stable limit cycle (thick solid curve). (b) Trajectories along the limit cycle for $x(t)$ (solid curve) and $q(t)$ (grey curve). Parameter values are $k_+ = 0.02, \gamma = 20, F_0 = 1$ and $h = -0.15$ with $k_- = 0.1$ in (b).

Let us begin our analysis by considering the deterministic network ($\epsilon = \sigma = 0$):

$$\frac{dq}{dt} = k_+(1-q) - k_- xq \tag{6.12}$$

$$\frac{dx}{dt} = -x + F(qx+h) \tag{6.13}$$

where we have set the membrane rate constant $\alpha = 1$. An equilibrium of the system (x^*, q^*) satisfies $q^* = k_+/(k_+ + k_- x^*)$ with x^* given by

$$x^* = F\left(\frac{k_+ x^*}{k_+ + k_- x^*} + h\right).$$

Let us assume that the network operates in a parameter regime where there exists a unique fixed point solution. By linearizing about the fixed point and calculating the eigenvalues of the Jacobian, we can find regimes where the fixed point destabilizes via a Hopf bifurcation leading to the formation of a limit cycle. An example bifurcation diagram is shown in Fig. 13 with the depletion rate k_- treated as the bifurcation parameter. Also shown are sample trajectories along the limit cycle.

6.2 Stochastic phase reduction

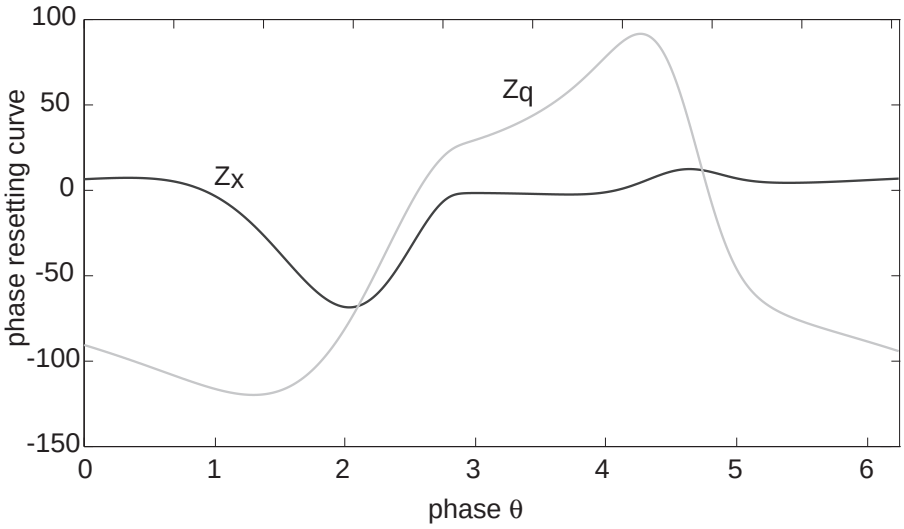

Figure 14: Components Z_x and Z_q of phase resetting curve for an excitatory network with synaptic depression. Same parameter values as Fig. 13(b).

Suppose that the deterministic network is operating in a limit cycle regime with natural frequency ω as shown in Fig. 13(b). Denote the corresponding limit cycle solution by $(x^*(\theta), q^*(\theta))$ with $\theta \in [-\pi, \pi)$. Following our analysis of the E-I network (section 4), we carry out a stochastic phase reduction. The first step is to convert the Ito term $b(X,Q)dW$ in equation (6.10) into a Stratonovich term:

$$\begin{aligned} dX &= \left[A(X,Q) - \frac{\epsilon^2}{2} b(X,Q) \frac{\partial b(X,Q)}{\partial X}\right] dt + \epsilon b(X,Q) dW(t) + \sigma a(X,Q) d\widehat{W}(t) \\ dQ &= [k_+(1-Q) - k_- XQ]dt. \end{aligned} \tag{6.14}$$

We then define a stochastic variable $\Theta = \Psi(X,Q)$, where Ψ is the associated isochronal mapping. The corresponding phase–reduced (Stratonovich) Langevin equation is

$$d\Theta = \omega + Z_x(\Theta) \left[-\frac{\epsilon^2}{2} b(\Theta) \partial b(\Theta) dt + \epsilon b(\Theta) dW(t) + \sigma a(\Theta) d\widehat{W}(t) \right] \tag{6.15}$$

where $Z_x(\theta)$ is the x–component of the infinitesimal phase resetting curve:

$$Z_x(\theta) = \left. \frac{\partial \Psi(x,q)}{\partial x} \right|_{x=x^*(\theta), q=q^*(\theta)}, \quad Z_q(\theta) = \left. \frac{\partial \Psi(x,q)}{\partial q} \right|_{x=x^*(\theta), q=q^*(\theta)} \tag{6.16}$$

with

$$Z_x(\theta)A(x^*(\theta),q^*(\theta))+Z_q(\theta)[k_+(1-q^*(\theta))-k_-x^*(\theta)q^*(\theta)]=\omega.$$

Also,

$$b(\theta)=b(x^*(\theta),q^*(\theta)),\quad \partial b(\theta)=\left.\frac{\partial b(x,q)}{\partial x}\right|_{x=x^*(\theta),q=q^*(\theta)},\quad a(\theta)=a(x^*(\theta),q^*(\theta)).$$

Finally, we convert to an Ito Langevin equation, which takes the compact form

$$d\Theta=\left[\omega-\frac{\epsilon^2}{2}\Omega(\Theta))+\frac{1}{4}\mathcal{B}'(\Theta)\right]dt+\epsilon\beta(\Theta)dW(t)+\sigma\alpha(\Theta)d\widehat{W}(t), \tag{6.17}$$

with

$$\Omega(\theta)=Z_x(\theta)b(\theta)\partial b(\theta),\quad \beta(\theta)=Z_x(\theta)b(\theta),\quad \alpha(\theta)=Z_x(\theta)a(\theta), \tag{6.18}$$

and

$$\mathcal{B}(\theta)=\sigma^2\alpha(\theta)^2+\epsilon^2\beta(\theta)^2 \tag{6.19}$$

6.3 Noise–induced synchronization

Now suppose that there exists an ensemble of $\mathcal{N}$ identical, uncoupled excitatory networks with synaptic depression labelled by μ, each with its own source of intrinsic noise and driven by a common source of extrinsic noise. Thus, after carrying out a stochastic phase reduction, each network evolves according to an Ito Langevin equation of the form (6.17):

$$d\Theta^{(\mu)}=\left[\omega-\frac{\epsilon^2}{2}\Omega(\Theta^{(\mu)}))+\frac{1}{4}\mathcal{B}'(\Theta^{(\mu)})\right]dt+\epsilon\beta(\Theta^{(\mu)})dW^{(\mu)}(t)+\sigma\alpha(\Theta^{(\mu)})d\widehat{W}(t) \tag{6.20}$$

for $\mu=1,\ldots,\mathcal{N}$. We associate an independent Wiener process $W^{(\mu)}$ with each excitatory network but take the extrinsic noise to be common to all populations. Thus,

$$\langle dW^{(\mu)}(t)dW^{(\nu)}(t)\rangle=\delta_{\mu,\nu}dt \tag{6.21}$$

$$\langle dW^{(\mu)}(t)d\widehat{W}(t)\rangle=0 \tag{6.22}$$

$$\langle d\widehat{W}(t)d\widehat{W}(t)\rangle=dt. \tag{6.23}$$

It follows that the ensemble is described by the multivariate Fokker–Planck equation (cf. equation (5.12))

$$\frac{\partial P(\boldsymbol{\theta},t)}{\partial t}=-\sum_{\mu=1}^{\mathcal{N}}\frac{\partial}{\partial\theta^\mu}[\mathcal{A}^{(\mu)}(\boldsymbol{\theta})P(\boldsymbol{\theta},t)]+\frac{1}{2}\sum_{\mu,\nu=1}^{\mathcal{N}}\frac{\partial^2}{\partial\theta^\mu\partial\theta^\nu}[C^{(\mu\nu)}(\boldsymbol{\theta})P(\boldsymbol{\theta},t)]. \tag{6.24}$$

with equal time correlation function

$$C^{(\mu\nu)}(\boldsymbol{\theta})=\sigma^2\alpha(\theta^{(\mu)})\alpha(\theta^{(\nu)})+\epsilon^2\beta(\theta^{(\mu)})\beta(\theta^{(\nu)})\delta_{\mu,\nu}, \tag{6.25}$$

drift term

$$\mathcal{A}^{(\mu)}(\boldsymbol{\theta}) = \omega - \frac{\epsilon^2}{2}\Omega(\theta^{(\mu)}) + \frac{1}{4}\mathcal{B}'(\theta^{(\mu)}), \tag{6.26}$$

and Ω etc. given by equations (6.18) and (6.19).

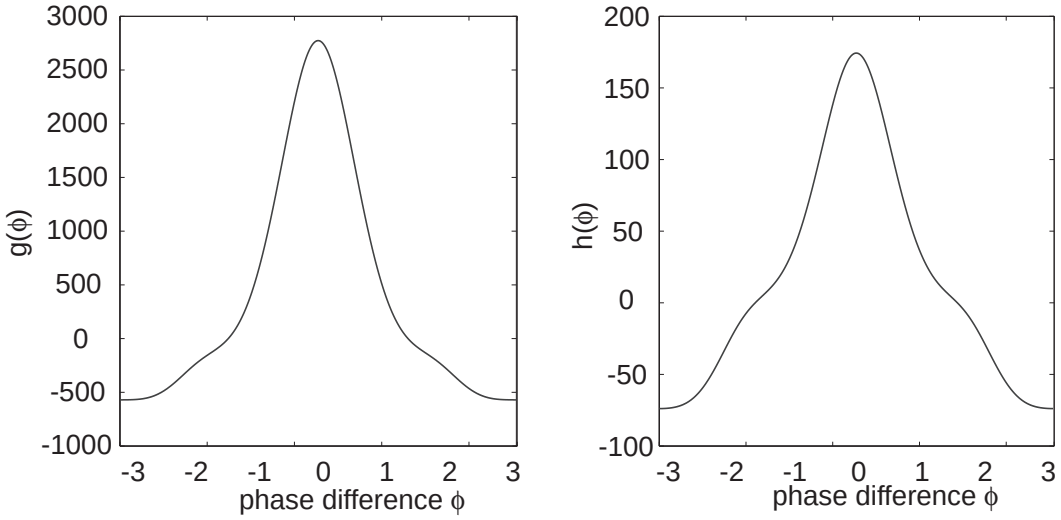

Figure 15: Plot of periodic functions g and h for an excitatory network with synaptic depression. Same parameters as Fig. 13(b).

Since equation (6.24) is identical in form to the FP equation (5.12) for the E-I network, we can carry out the averaging procedure detailed in section 5. The final result of this analysis is the steady state distribution $\Phi_0(\phi)$ for the phase difference ϕ of any pair of oscillators given by equation (5.23) with

$$g(\psi) = \frac{1}{2\pi}\int_{-\pi}^{\pi} \alpha(\theta')\alpha(\theta'+\psi)d\theta' \tag{6.27}$$

$$h(\psi) = \frac{1}{2\pi}\int_{-\pi}^{\pi} \beta(\theta')\beta(\theta'+\psi)d\theta' \tag{6.28}$$

and α, β given by equation (6.18). An example plot of the periodic functions $g(\psi), h(\psi)$ for an excitatory network with synaptic depression is given in Fig. 15. In Fig. 16 we plot an example of the distribution Φ_0 illustrating how, as in the case of an E-I network, the synchronizing effects of a common extrinsic noise source are counteracted by the uncorrelated intrinsic noise arising from finite-size effects.

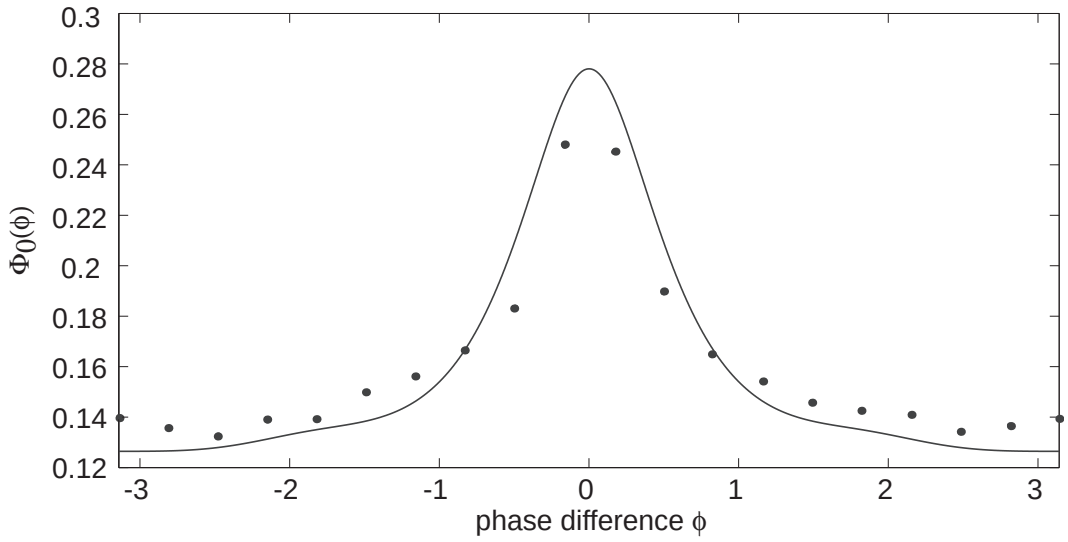

Figure 16: Probability distribution of the phase difference between a pair of excitatory networks with synaptic depression with g, h given by Fig. 15. Solid curves are based on analytical calculations, whereas black filled circles correspond to stochastic simulations of the phase–reduced Langevin equation. Same parameters as Fig. 13(b).

7 Discussion

In this paper we extended the theory of noise–induced synchronization to a stochastic Wilson–Cowan model of neural population dynamics formulated as a neural master equation. We considered two canonical network structures that are known to exhibit limit cycle oscillations in the deterministic limit; an E-I network of mutually interacting excitatory and inhibitory populations, and an excitatory network with synaptic depression. In both cases, we used phase reduction methods and averaging theory to explore the effects of intrinsic noise on the synchronization of uncoupled limit cycle oscillators driven by a common extrinsic noise source. We achieved this by first approximating the neural master equation by a corresponding neural Langevin equation. Such an approximation is reasonable for sufficiently large system size N, and provided that there do not exist other stable attractors of the deterministic system [9]. One important consequence of intrinsic noise is that it leads to a multiplicative form of uncorrelated noise in the corresponding Langevin equation, which broadens the distribution of phase differences. The degree of broadening depends on the term $N^{-1}h(0)$, see equation (5.23), where N is the system size N and $h(0)$ depends on the intrinsic dynamics of each uncoupled limit cycle oscillator, as expressed by the phase resetting curve, and the particular form of the multiplicative noise, see

equations (5.6), (5.17), (6.18) and (6.28).

It is important to point out that the master equation formulation of stochastic neurodynamics developed here and elsewhere [13, 14, 8, 9] is a phenomenological representation of stochasticity at the population level. It is not derived from a detailed microscopic model of synaptically coupled spiking neurons, and it is not yet clear under what circumstances such a microscopic model would yield population activity consistent with the master equation approach. Nevertheless, if one views the Wilson–Cowan rate equations [69, 70] as an appropriate description of large-scale neural activity in the deterministic limit, it is reasonable to explore ways of adding noise to such equations from a top–down perspective. One possibility is to consider a Langevin version of the Wilson–Cowan equations involving some form of extrinsic additive white noise [32, 21], whereas another is to view the Wilson–Cowan rate equations as the thermodynamic limit of an underlying master equation that describes the effects of intrinsic noise [13, 14, 8, 51]. As we have highlighted in this paper, the latter leads to a multiplicative rather than additive form of noise.

There are a number of possible extensions of this work. First, one could consider more complicated network architectures that generate limit cycle oscillations at the population level. One particularly interesting example is a competitive network consisting of two excitatory populations with synaptic depression (or some other form of slow adaptation) that mutually inhibit each other. Such a network has recently been used to model noise–induced switching during binocular rivalry [39, 68, 42, 56, 57, 36]. Binocular rivalry concerns the phenomenon whereby perception switches back and forth between different images presented to either eye [3, 4]. Experimentally, it has been found that the eye dominance time statistics may be fit to a gamma distribution, suggesting that binocular rivalry is driven by a stochastic process [41]. One possibility is that there is an extrinsic source of noise associated with the input stimuli. A number of recent models have examined dominance switching times due to additive noise in a competitive Wilson–Cowan model with additional slow adapting variables [42, 56, 57]. On the other hand, Laing and Chow [39] considered a deterministic spiking neuron model of binocular rivalry in which the statistics of the resulting dominance times appeared noisy due to the aperiodicity of the high–dimensional system's trajectories. The latter is suggestive of an effective intrinsic noise source within a rate–based population model. A second extension of our work would be to introduce synaptic coupling between the limit cycle oscillators. For example, in the case of E-I networks such coupling could represent intracortical connections between columns in visual cortex [60, 28]. The effects of mutual coupling on noise–induced synchronization has been explored within the context of a pair of coupled conductance–based neurons [43].

Acknowledgements

This publication was based on work supported in part by the National Science Foundation (DMS-0813677) and by Award No KUK-C1-013-4 made by King Abdullah University of Science and Technology (KAUST). PCB was also partially supported by the Royal Society Wolfson Foundation.

References

[1] L F Abbott and C van Vresswijk. Asynchronous states in networks of pulse–coupled oscillators. Phys. Rev. E, 48: 1483–1490, 1993.

[2] L F Abbott, J A Varela, K Sen and S BNelson. Synaptic depression and cortical gain control. Science 275: 220–224, 1997.

[3] R Blake, A primer on binocular rivalry, including current controversies, Brain and Mind, 2: 5–38, 2001.

[4] R Blake and N Logothetis. Visual competition. Nat. Rev. Neurosci. 3: 13–23, 2002.

[5] R P Boland, T Galla and A J McKane How limit cycles and quasi-cycles are related in systems with intrinsic noise. J. Stat. Mech., 9: P09001, 2008.

[6] R Borisyuk and A B Kirillov. Bifurcation analysis of a neural network model. Biol. Cybern, 66: 319–325, 1992

[7] S El Boustani and A Destexhe. A master equation formalism for macroscopic modeling of asynchronous irregular activity states. Neural Comput, 21: 46–100, 2009.

[8] P C Bressloff. Stochastic neural field theory and the system-size expansion. SIAM J. Appl. Math, 70: 1488–1521, 2009.

[9] P C Bressloff. Metastable states and quasicycles in a stochastic Wilson-Cowan model of neuronal population dynamics. Phys. Rev. E. In press, 2010.

[10] N Brunel. Dynamics of sparsely connected networks of excitatory and inhibitory spiking neurons. J Comput. Neurosci, 8: 183–208, 2000.

[11] N Brunel and V Hakim. Fast global oscillations in networks of integrate–and–fire neurons with low firing rates. Neural Comput., 11: 1621–1671, 1999.

[12] E Buckwar and M G Riedler. An exact stochastic hybrid model of excitable membranes including spatio-temporal evolution. J. Math. Biol. In press, 2010.

[13] M Buice and J D Cowan. Field-theoretic approach to fluctuation effects in neural networks. Phys. Rev. E, 75: 051919, 2007.

[14] M Buice, J D Cowan, and C C Chow. Systematic fluctuation expansion for neural network activity equations. Neural Comput., 22: 377–426, 2010.

[15] G Buzsaki. *Rhythms of the Brain*. Oxford University Press, Oxford, 2006.

[16] Y Cao, D T Gillespie, and L R Petzold. Avoiding negative populations in explicit Poisson tau-leaping. J. Chem. Phys., 123: 054104, 2005.

[17] Y Cao, D T Gillespie, and L R Petzold. Adaptive explicit-implicit tau-leaping method with automatic tau selection. J. Chem. Phys., 126: 224101, 2007.

[18] B Doiron, B Lindner B, A Longtin, L Maler and J Bastian. Oscillatory activity in electrosensory neurons increases with the spatial correlation of the stochastic input stimulus. Phys. Rev. Lett. 93: 048101, 2004.

[19] G B Ermentrout. Noisy Oscillators. In: *Stochastic methods in neuroscience.* C R Laing and G J Lord (eds.), Oxford University Press, 2009.

[20] G B Ermentrout and N Kopell. Multiple pulse interactions and averaging in coupled neural oscillators, J. Math. Biol. 29: 195–217, 1991.

[21] O Faugeras, J Touboul and B Cessac. A constructive mean–field analysis of multi–population neural networks with random synaptic weights and stochastic inputs. Frontiers in Comp. Neurosci. **3:** 1–28 (2009).

[22] R F Galan, G B Ermentrout and N N Urban. Correlation-induced synchronization of oscillations in olfactory bulb neurons. J. Neurosci. 26: 3646–3655, 2006.

[23] R F Galan, G B Ermentrout and N N Urban. Optimal time scale for spike-time reliability: theory, simulations and expeiments. J. Neurophysiol. 99: 277–283, 2008.

[24] C Gardiner. *Stochastic Methods.* 4th Edition, Springer, Berlin, 2009

[25] W Gerstner and J L Van Hemmen. Coherence and incoherence in a globally coupled ensemble of pulse–emitting units. Phys. Rev. Lett., 71: 312–315, 1993.

[26] D T Gillespie. The chemical Langevin equation. J. Chem. Phys. 113: 297–306, 2000.

[27] D S Goldobin and A Pikovsky. Synchronization and desynchronization of self–sustained oscillators by common noise. Phys. Rev. E 71: 045201, 2005.

[28] E R Grannan, D Kleinfeld, and H Sompolinsky. Stimulus-dependent synchronization of neuronal assemblies. Neural Comput. 5: 550–569, 1993.

[29] C M Gray. The temporal correlation hypothesis of visual feature integration: still alive and well. Neuron, 24: 31–47, 1999.

[30] A Guillamon and G Huguet. A computational and geometric approach to phase resetting curves and surfaces. SIAM J. Appl. Dyn. Syst., 8: 1005–1042, 2009.

[31] D Holcman and M Tsodyks. The emergence of Up and Down states in cortical networks. PLoS Comput. Biol. 2: 174–181, 2006.

[32] A Hutt, A Longtin and L Schimansky-Geier. Additive noise–induced Turing transitions in spatial systems with application to neural fields and the Swift–Hohenberg equation Physica D **237**: 755–773 (2008).

[33] N G Van Kampen. *Stochastic processes in physics and chemistry.* North-Holland, Amsterdam, 1992.

[34] Z P Kilpatrick and P C Bressloff. Effects of synaptic depression and adaptation on spatiotemporal dynamics of an excitatory neuronal network. Physica D.239: 547–560, 2010.

[35] Z P Kilpatrick and P C Bressloff. Spatially structured oscillations in a two–dimensional excitatory neuronal network with synaptic depression. J. Comput. Neurosci. 28: 193–209, 2010.

[36] Z P Kilpatrick and P C Bressloff. Binocular rivalry in a competitive neural network with synaptic depression. SIAM J. Appl. Dyn. Syst. In press, 2010.

[37] Y Kuramoto. *Chemical oscillations, waves and turbulence* Springer, Berlin, 1984.

[38] T G Kurtz. Limit theorems and diffusion approximations for density dependent Markov chains. Math.Prog. Stud. 5: 67, 1976.

[39] C R Laing and C C Chow. A spiking neuron model for binocular rivalry. J. Comput. Neurosci. 12: 39–53, 2002.

[40] J Lei. Stochasticity in single gene expression with both intrinsic noise and fluctuations in kinetic parameters. J. Theor. Biol. 256: 485–492, 2009.

[41] N K Logothetis, D A Leopold, and D L Sheinberg. What is rivalling during binocular rivalry? Nature 380: 621–624 , 1996.

[42] R Moreno-Bote, J Rinzel, and N Rubin. Noise–induced alternations in an attractor network model of perceptual bistability. J. Neurophysiol. 98: 1125–1139, 2007.

[43] C Ly and G B Ermentrout. Synchronization of two coupled neural oscillators receiving shared and unshared noisy stimuli. J. Comput. Neurosci. 26: 425-443, 2009.

[44] Z F Mainen and T J Sejnowski. Reliability of spike timing in neocortical neurons. Science 268: 1503–1506, 1995.

[45] S Marella and G B Ermentrout. Class-II neurons display a higher degree of stochastic synchronization than class-I neurons. Phys. Rev. E 77: 41918, 2008.

[46] M Mattia and P Del Guidice. Population dynamics of interacting spiking neurons. Phys. Rev. E, 66: 051917, 2002.

[47] A J McKane, J D Nagy, T J Newman and M O Stefanini Amplified biochemical oscillations in cellular systems J. Stat. Phys. 71: 165–191, 2007

[48] C Meyer and C van Vreeswijk. Temporal correlations in stochastic networks of spiking neurons. Neural Comput. 14: 369–404, 2002.

[49] H Nakao, K Arai and Y Kawamura. Noise-induced synchronization and clustering in ensembles of uncoupled limit cycle oscillators. Phys. Rev. Lett. 98: 184101, 2007.

[50] W H Nesse, A Borisyuk and P C Bressloff. Fluctuation-driven rhythmogenesis in an excitatory neuronal network with slow adaptation. J. Comput. Neurosci. 25: 317–333, 2008.

[51] T Ohira and J D Cowan. Stochastic neurodynamics and the system size expansion. In S Ellacott and I J Anderson, editors, *Proceedings of the first international conference on Mathematics of neural networks*, pages 290–294. Academic Press, 1997.

[52] K Pakdaman, M Thieullen and G Wainrib. Fluid limit theorems for stochastic hybrid systems with application to neuron models. Adv. Appl. Probab. 42: 761–794 (2010).

[53] A S Pikovsky. Synchronization and stochastization of an ensemble of autogenerators by external noise. Radiophys. Quantum Electron. 27: 576–581, 1984.

[54] A Renart, N Brunel, and X-J Wang. Mean–field theory of irregularly spiking neuronal populations and working memory in recurrent cortical networks. In J. Feng, editor, *Computational Neuroscience: a comprehensive approach*, pp. 431–490. CRC Press, Boca Raton, Fl, 2004.

[55] E Salinas and T J Sejnowski. Correlated neuronal activity and the flow of neural information. Nature Rev. Neurosci., 4: 539–550, 2001.

[56] A Shpiro, R Curtu, J Rinzel, and N Rubin. Dynamical characteristics common to neuronal competition models. J Neurophysiol. 97: 462–473, 2007.

[57] A Shpiro, R. Moreno-Bote, N. Rubin, and J. Rinzel. Balance between noise and adaptation in competition models of perceptual bistability. J. Comp. Neurosci 27: 37–54, 2009.

[58] W Singer and C M Gray. Visual feature integration and the temporal correlation hypothesis. Annu Rev Neurosci 18: 555–586, 1995.

[59] T J Sejnowski and O Paulsen. Network oscillations: Emerging computational principles. J. Neurosci. 26: 1673–1676, 2006.

[60] H G Shuster and P Wagner. A model for neuronal oscillations in the visual cortex. Biol. Cybern, 64: 77-82, 1990.

[61] H Soula and C C Chow. Stochastic dynamics of a finite-size spiking neural network. Neural Comput, 19: 3262–3292, 2007.

[62] J Tabak, W Senn, M J O'Donovan and J Rinzel. Modeling of spontaneous activity in developing spinal cord using activity-dependent depression in an excitatory network. J. Neurosci. 20: 3041–3056, 2000.

[63] J Tabak, M J O'Donovan and J Rinzel Differential control of active and silent phases in relaxation models of neuronal rhythms. J Comp. Neurosci 21: 307–328, 2006.

[64] J-N Teramae and D Tanaka. Robustness of the noise-induced phase synchronization in a general class of limit cycle oscillators. Phys. Rev. Lett. 93: 204103, 2007.

[65] J-N Teramae, H Nakao and G B Ermentrout. Stochastic phase reduction for a general class of noisy limit cycle oscillators. Phys. Rev. Lett. 102: 194102, 2009.

[66] M S Tsodyks, K Pawelzik and H Markram. Neural networks with dynamic synapses. Neural Comput. 10: 821–835, 1998.

[67] B Vladimirski, J Tabak, M J O'Donovan and J Rinzel. Episodic activity in a heterogeneous excitatory network, from spiking neurons to mean field. J. Comput. Neurosci. 25: 39–63, 2008.

[68] H R Wilson. Computational evidence for a rivalry hierarchy in vision. Proc Natl Acad Sci USA 100: 14499–14503, 2003.

[69] H R Wilson and J D Cowan. Excitatory and inhibitory interactions in localized populations of model neurons. Biophys. J., **12:** 1–23, 1972.

[70] H R Wilson and J D Cowan. A mathematical theory of the functional dynamics of cortical and thalamic nervous tissue. Kybernetik, 13: 55–80, 1973.

[71] S Zeisler , U Franz, O Wittich and V Liebscher. Simulation of genetic networks modelled by piecewise deterministic Markov processes. IET Syst. Bio. 2: 113–135, 2008.

RECENT REPORTS

37/10	Circumferential buckling instability of a growing cylindrical tube	Moulton Goriely
38/10	Preconditioners for state constrained optimal control problems with Moreau-Yosida penalty function	Stoll Wathen
39/10	Local synaptic signaling enhances the stochastic transport of motor-driven cargo in neurons	Newby Bressloff
40/10	Convection and Heat Transfer in Layered Sloping Warm-Water Aquifer	McKibbin Hale Style Walters
41/10	Optimal Error Estimates of a Mixed Finite Element Method for Parabolic Integro-Differential Equations with Non Smooth Initial Data	Goswami Pani Yadav
42/10	On the Linear Stability of the Fifth-Order WENO Discretization	Motamed Macdonald Ruuth
43/10	Four Bugs on a Rectangle	Chapman Lottes Trefethen
44/10	Mud peeling and horizontal crack formation in drying clay	Style Peppin Cocks
45/10	Binocular Rivalry in a Competitive Neural Network with Synaptic Depression	Kilpatrick Bressloff
46/10	A theory for the alignment of cortical feature maps during development	Bressloff Oster
47/10	All-at-Once Solution if Time-Dependent PDE-Constrained Optimisation Problmes	Stoll Wathen
48/10	Possible role of differential growth in airway wall remodeling in asthma	Moulton Goriely
49/10	Variational Data Assimilation Using Targetted Random Walks	Cotter Dashti Robinson Stuart
50/10	A model for the anisotropic response of fibrous soft tissues using six discrete fibre bundles	Flynn Rubin Nielsen
51/10	STOCHSIMGPU Parallel stochastic simulation for the Systems Biology Toolbox 2 for MATLAB	Klingbeil Erban Giles Maini

52/10	Order parameters in the Landau-de Gennes theory - the static and dynamic scenarios	Majumdar
53/10	Liquid Crystal Theory and Modelling Discussion Meeting	Majumdar Mottram
54/10	Modeling the growth of multicellular cancer spheroids in a bioengineered 3D microenvironment and their treatment with an anticancer drug	Loessner Flegg Byrne Hall Moroney Clements Hutmacher McElwain
55/10	Scalar Z, ZK, KZK, and KP equations for shear waves in incompressible solids	Destrade Goriely Saccomandi
56/10	The Influence of Bioreactor Geometry and the Mechanical Environment on Engineered Tissues	Osborne ODea Whiteley Byrne Waters
57/10	A numerical guide to the solution of the bidomain equations of cardiac electrophysiology	Pathmanathan Bernabeu Bordas Cooper Garny Pitt-Francis Whiteley Gavaghan
58/10	Particle-scale structure in frozen colloidal suspensions from small angle X-ray scattering	Spannuth Mochrie Peppin Wettlaufer
59/10	Spin coating of an evaporating polymer solution	Munch Please Wagner

Copies of these, and any other OCCAM reports can be obtained from:

Oxford Centre for Collaborative Applied Mathematics
Mathematical Institute
24 - 29 St Giles'

Oxford
OX1 3LB
England
www.maths.ox.ac.uk/occam